Lithos 108 (2009) 106–125

Contents lists available at ScienceDirect

Lithos

journal homepage: www.elsevier.com/locate/lithos

Late Cretaceous intra-oceanic magmatism in the internal Dinarides (northern Bosnia and Herzegovina): Implications for the collision of the Adriatic and European plates

Kamil Ustaszewski [a,*], Stefan M. Schmid [a], Boško Lugović [b], Ralf Schuster [c], Urs Schaltegger [d], Daniel Bernoulli [a], Lukas Hottinger [a], Alexandre Kounov [a], Bernhard Fügenschuh [e], Senecio Schefer [a]

[a] Institute of Geology and Paleontology, Bernoullistrasse 32, University of Basel, CH-4056 Basel, Switzerland
[b] Rudarsko-geološko-naftni fakultet, HR-10000 Zagreb, Croatia
[c] Geologische Bundesanstalt, A-1030 Wien, Austria
[d] Département de Minéralogie, CH-1205 Genève, Switzerland
[e] Geologisch-Paläontologisches Institut, A-6020 Innsbruck, Austria

ARTICLE INFO

Article history:
Received 17 September 2007
Accepted 17 September 2008
Available online 7 October 2008

Keywords:
Ophiolites
Sm–Nd-dating
U–Pb dating
Geochemistry
Dinarides
Vardar Ocean

ABSTRACT

The Kozara Mountains of northern Bosnia and Hercegovina form part of the internal Dinarides and host two tectonically juxtaposed ophiolitic successions of different age. The southern part of the Kozara Mountains exposes the Western Vardar Ophiolitic Unit, which was obducted onto the Adriatic margin in the Late Jurassic. The northern part exposes a bimodal igneous succession that was thrust onto the Western Vardar Ophiolitic Unit during the latest Cretaceous to Early Paleogene. This bimodal igneous succession comprises isotropic gabbros, doleritic dikes, basaltic pillow lavas and rhyolites. Pelagic limestones, intercalated with pillow lavas, yielded a Campanian globotruncanid association, consistent with concordant U–Pb ages on zircons from dolerites and rhyolites of 81.39±0.11 and 81.6±0.12 Ma, respectively.

Chondrite-normalised rare earth element patterns of the bimodal igneous rocks show enrichment of LREE over HREE. Primitive mantle-normalised multi-element diagrams do not reveal significant depletion of HFSE. The εNd(T) and initial $^{87}Sr/^{86}Sr$ isotopic values range from +4.4 to +6.3 and from 0.70346 to 0.70507 respectively, suggesting an intraoceanic origin.

The bimodal igneous succession is unconformably overlain by Maastrichtian to Paleocene siliciclastics that contain abundant ophiolitic detritus, suggesting reworking of the Campanian magmatics. An Eocene turbiditic sandstone succession unconformably covers both the Western Vardar Ophiolitic Unit and the Late Cretaceous bimodal igneous successions. These observations suggest that the Adriatic Plate and the Europe-derived Tisza and Dacia Mega-Units were still separated by a deep basin floored by oceanic lithosphere until the Campanian and that its closure did not occur before the Maastrichtian to earliest Paleogene. This Late Cretaceous oceanic domain probably represented a remnant of the Vardar Ocean, or alternatively, the Alpine Tethys; possibly the traces of both oceanic domains were connected in the area.

1. Introduction

1.1. Large-scale tectonic setting

The widespread occurrence of ophiolites is one of the most distinctive features of the Dinarides and Hellenides of the Balkan Peninsula. They can be traced for about 1000 km along strike, from the area of Zagreb (Croatia) in the northwest to the Peloponnesus (Greece) in the southeast and beyond (Fig. 1). In map view, the ophiolites exposed west of a line Zagreb–Beograd–Skopje form two parallel, spatially separate belts (Smith and Spray, 1984). Petrographic and geochemical differences between the ophiolites of the two belts were used as evidence for the existence of two distinct oceanic basins, originally separated by one or several Adria-derived micro-continents that included the Drina-Ivanjica, Jadar and Pelagonian blocks (Robertson and Karamata, 1994; Dimitrijević, 1997, 2001; Karamata, 2006; Dilek et al., 2008). This 'two ocean' model contrasts with that of Bernoulli and Laubscher (1972), Smith and Spray (1984) and Pamić et al. (2002), who suggested an origin of both ophiolitic belts in one ocean. Schmid et al. (2008) support the 'single ocean' model and consider the two belts of ophiolites as relics of the same, formerly coherent ophiolitic sheet (their Western Vardar Ophiolitic Unit) that was obducted onto the Adriatic passive margin in the Late Jurassic and was disrupted by Cretaceous to Tertiary thrusting. Thrusting has exposed units derived from the Adriatic margin below the ophiolitic units in the form of windows, which were interpreted as micro-continents by earlier authors (Fig. 1).

* Corresponding author. Now at: Department of Geosciences, National Taiwan University, 10617 Taipei, Taiwan.
E-mail address: kamilu@ntu.edu.tw (K. Ustaszewski).

0024-4937/$ – see front matter © 2008 Elsevier B.V. All rights reserved.
doi:10.1016/j.lithos.2008.09.010

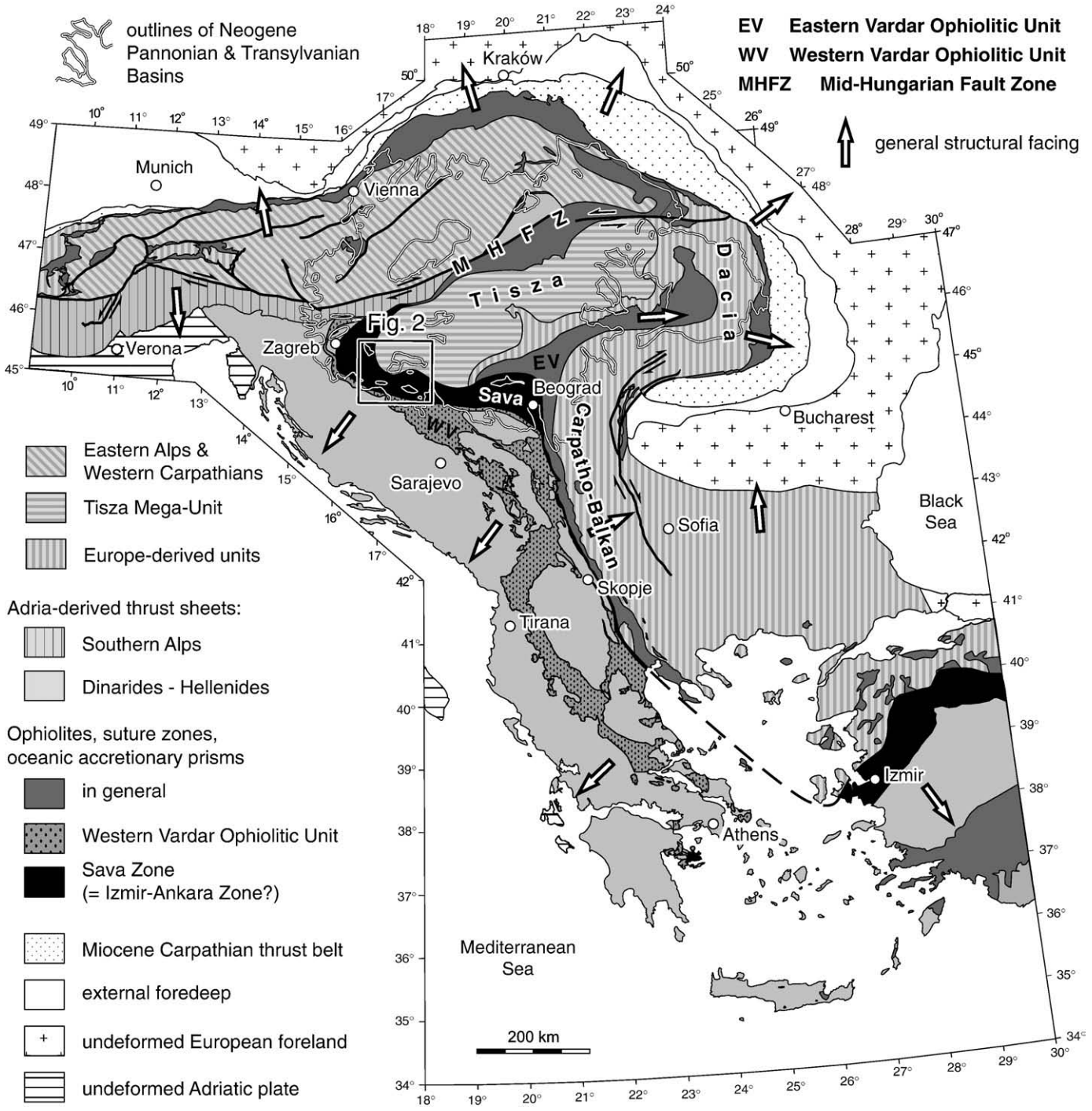

Fig. 1. Major tectonic units of the Alps, Carpathians, Dinarides and Hellenides (north of 42°N, simplified after Schmid et al., 2008).

The spatial separation of these ophiolitic belts gave rise to a number of different names. The western (external) belt is referred to as Dinaride (or Dinaridic) ophiolite belt (Robertson and Karamata, 1994; Pamić et al., 2002), or as the Central Dinaridic ophiolite belt (Lugović et al., 1991). The eastern (internal) belt has a variety of names: Western Vardar ophiolites (Karamata, 2006), Inner Dinaridic ophiolite belt (Lugović et al., 1991), External Vardar Subzone (Dimitrijević, 1997, 2001) or simply Vardar Zone (Robertson and Karamata, 1994; Pamić et al., 2002). The terminology adopted here follows that of Schmid et al. (2008), who refer to the two belts located west and east of the Drina-Ivanjica unit as Dinaridic and Western Vardar ophiolites, respectively, in a structural sense. Since Schmid et al. (2008) regard the two ophiolitic belts as having formed in the same ocean, they use "Western Vardar Ophiolitic Unit" (WV; Fig. 1) when collectively referring to both the ophiolite belts and the ocean from which the ophiolites were derived. There is yet another ophiolitic branch of the Vardar Ocean, located further to the east, referred to as the Eastern Vardar Ophiolitic Unit (Fig. 1).

1.2. When did the Vardar Ocean close?

A controversial topic is the time of the closure of the Vardar Ocean that led to collision of Adria with smaller Europe-derived plates like the

Tisza and Dacia Mega-Units (see Schmid et al., 2008 and references therein). The different branches of the Vardar Ocean (and the Alpine Tethys) were involved in two orogens of different age and structural facing direction: 1) the Early to middle Cretaceous, Europe-vergent South Carpathians (Dacia Mega-Unit) including the Carpatho-Balkan orogen in the NE, and 2) the SW-vergent Dinarides, which, with the obducted Western Vardar Ophiolitic Unit, form the NE edge of the Adriatic Plate (Fig. 1). The Tisza Mega-Unit, located NE of the Vardar suture, referred to as Sava Zone by Schmid et al. (2008), was originally separated from the Dacia Mega-Unit by another oceanic branch represented by the Eastern Vardar Ophiolitic Unit. The Tisza and Dacia Mega-Units were juxtaposed along the East-Vardar suture in the late Early Cretaceous (Săndulescu and Visarion, 1977). The West-Vardar suture, i.e. the consumed oceanic domain between Tisza–Dacia on the one hand and Adria on the other hand, belonged to a branch of the Triassic to Jurassic Meliata–Maliac–Vardar Ocean (Schmid et al., 2008), part of the Neotethys *sensu* Ricou (1994). The Neotethys was probably linked to the Alpine Tethys somewhere in the area around Zagreb. For simplicity, we use the name Vardar Ocean for this ocean that closed to form the Sava Zone suture. The closure of this ocean was hitherto inferred to have occurred in the Late Cretaceous–Early Paleogene, based on the following observations:

a.) Blueschist-facies metamorphosed metabasalts in Fruška Gora (N of Beograd) yielded glaucophane K–Ar ages of 123±5 Ma (Milovanović et al., 1995). They are believed to mark subduction of oceanic lithosphere of the Vardar Ocean ongoing at that time.

b.) The stratigraphic minimum age of strongly deformed, very low- to low-grade metamorphosed sediments in the most internal Dinarides, containing olistoliths of mafics and ultramafics as well as tectonically incorporated Mesozoic platform carbonates, is Late Cretaceous ("Senonian" flysch of Dimitrijević, 1997; Pamić, 2002; Schefer et al., 2007).

c.) A belt of Late Cretaceous, mainly calc-alkaline igneous rocks, stretching from central Bulgaria across eastern Serbia into western Romania, is informally referred to as "banatites". They are mostly associated with Late Cretaceous (Turonian to Campanian age, 92–78 Ma) volcano-sedimentary basins and are interpreted to have formed in a back-arc setting related to the N- to NE-directed subduction of the Vardar Ocean beneath Europe-derived units (e.g. Georgiev et al., 2001; Heinrich and Neubauer, 2002; Neubauer et al., 2003; von Quadt et al., 2005).

d.) Greenschist- to amphibolite-facies metapelites in North Bosnia (Pamić and Prohić, 1989; Pamić, 1993a) with a biostratigraphically determined Maastrichtian protolith age (Pantić and Jovanović 1970; Šparica et al., 1980, 1984; Jovanović and Magaš 1986) are thought to mark a post-collisional metamorphic event (Pamić, 2002).

In Central Serbia, the surface expression of the Sava Zone suture is a N–S-trending, few kilometre wide belt of Late Cretaceous ("Senonian") flysch. At the latitude of Beograd this suture bends into an E–W trend and opens into a 50 km wide corridor parallel to the Sava River (therefore termed Sava Zone, Fig. 1, corresponding to the "Northwestern Vardar Zone" of Pamić, 1993a, or the "Sava–Vardar Zone" of Pamić, 2002). Between Beograd and Zagreb the suture is exposed in a few isolated inselbergs located at the southwestern margin of the Pannonian Basin (Fig. 2).

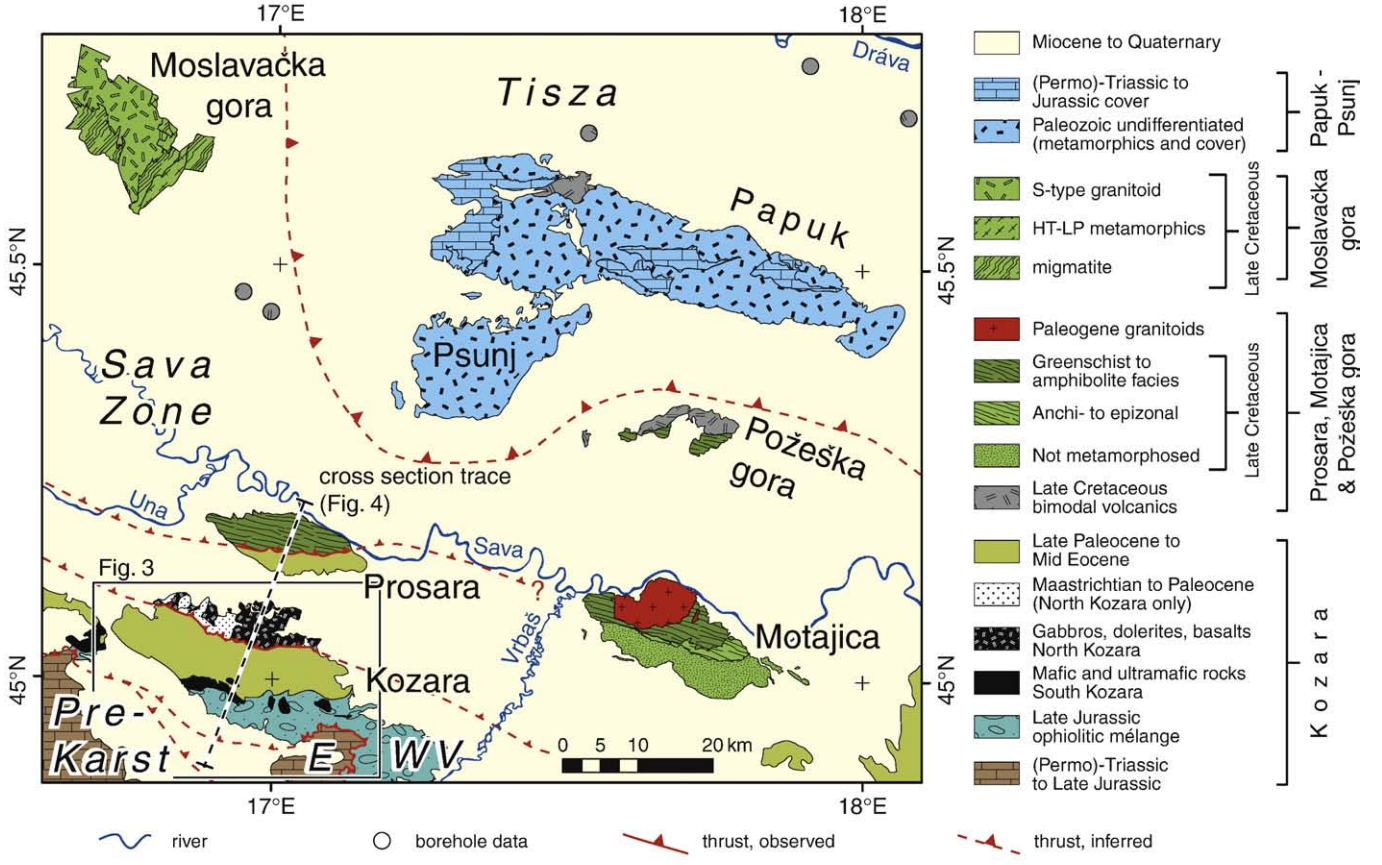

Fig. 2. Simplified geologic–tectonic map of the study area, compiled from 1:100,000 map sheets of former Yugoslavia (referenced in the text) and Pamić et al. (2000). Well locations are from Pamić (1997). Tectonic contacts between major tectonic units (in italics) are from Schmid et al. (2008). Only inferred Paleogene and older contacts are shown, while faults related to the Neogene extension of the Pannonian Basin are neglected. WV=Western Vardar Ophiolitic Unit, E=East–Bosnian–Durmitor unit.

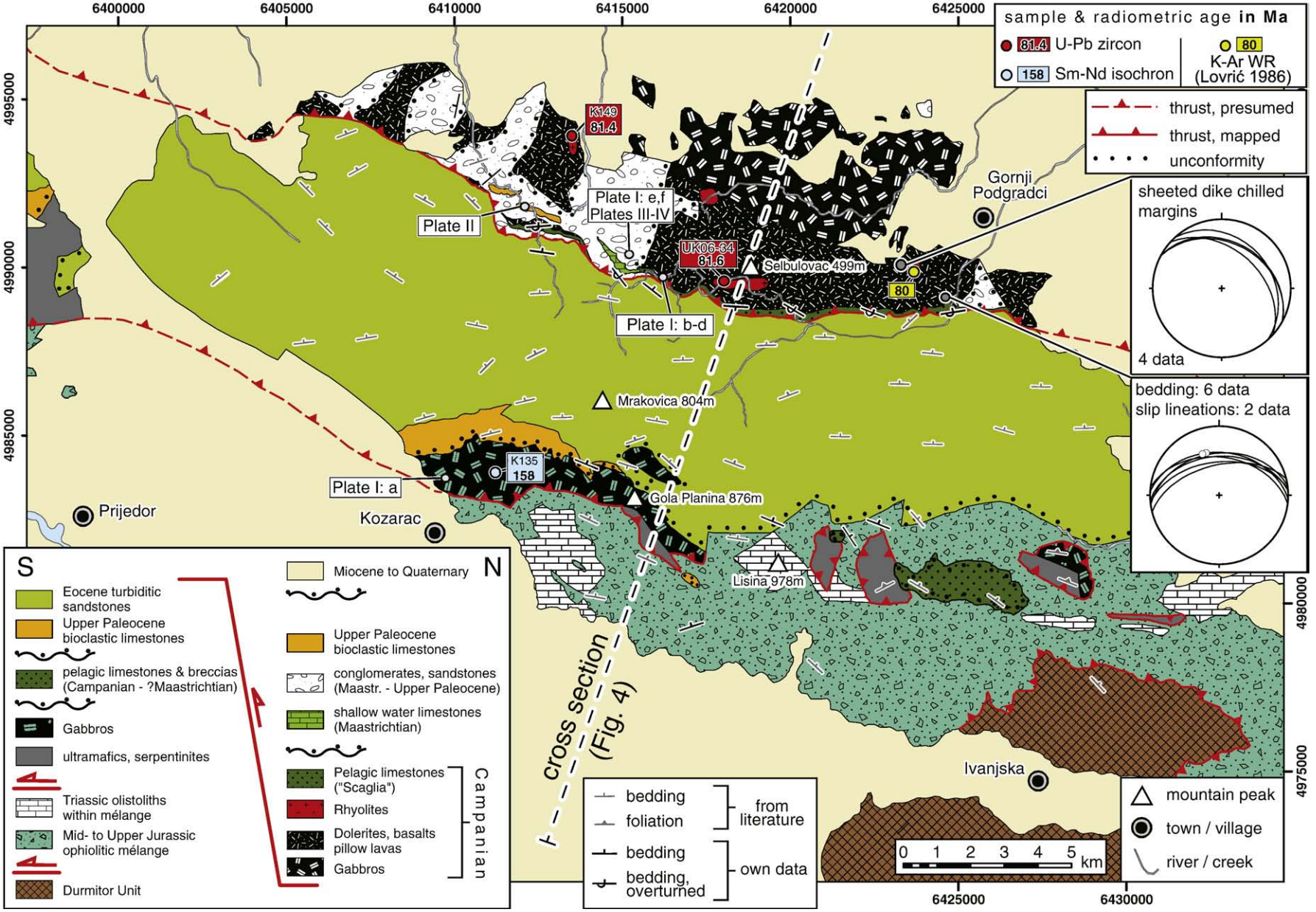

Fig. 3. Geological map of the Kozara Mountains, compiled from 1:100,000 geological map sheets of former Yugoslavia (see text for references) and modified according to own observations. Numbers at the edges of the map are MGI Balkan 6 Cartesian coordinates. Structural data plotted at the right edge are lower hemisphere, equal area projections.

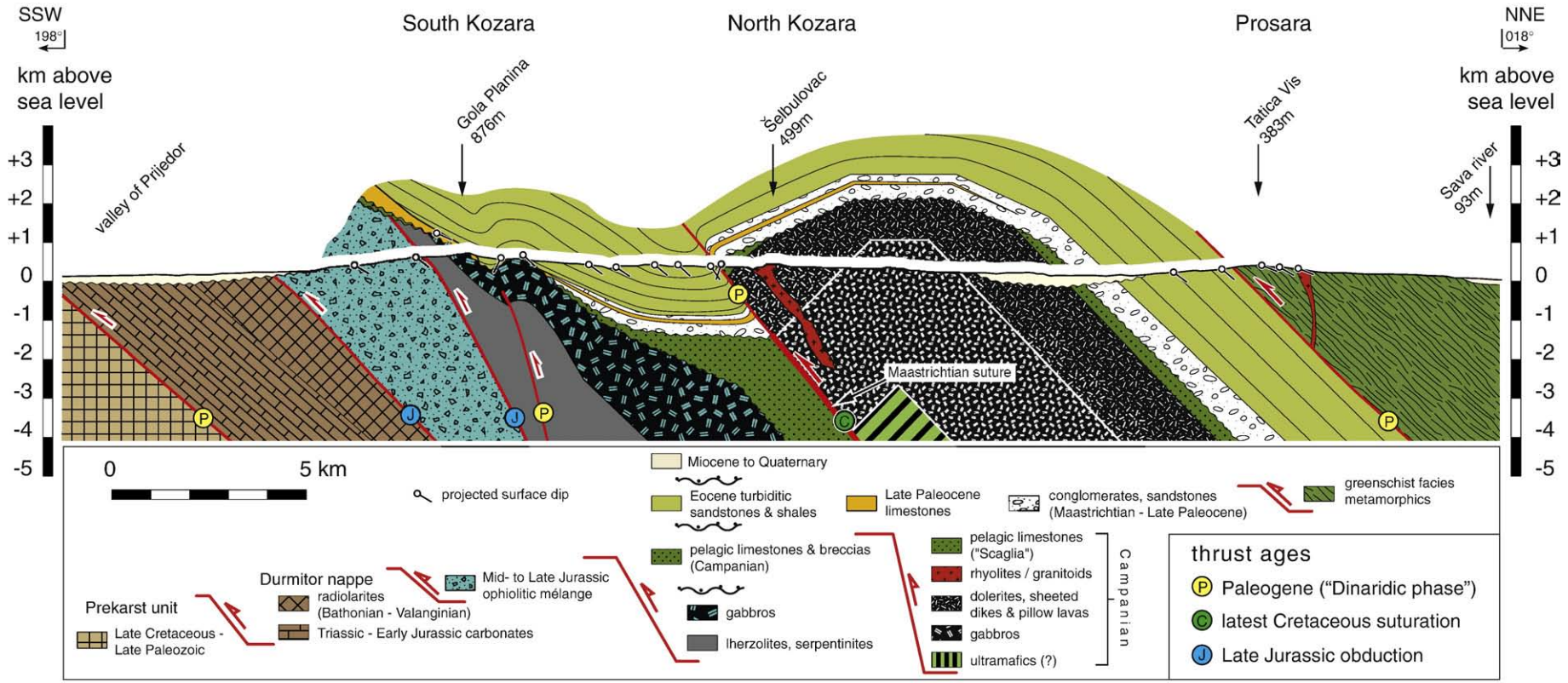

Fig. 4. Geological cross-section across the Kozara and Prosara Mountains. See Figs. 2 and 3 for location.

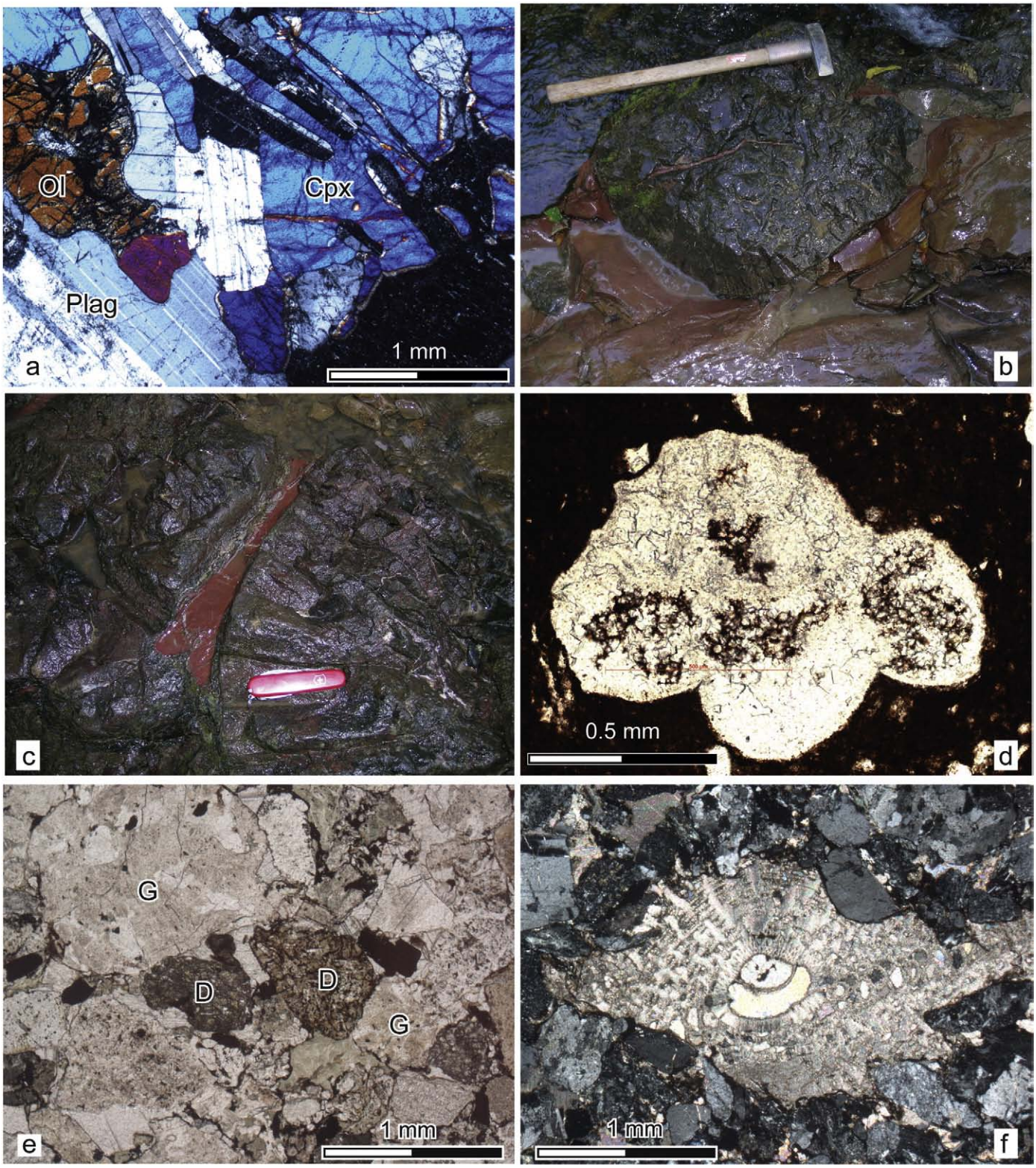

Plate I.

a. Thin-section photomicrograph of an olivine-bearing cumulate gabbro (sample K135) from South Kozara, selected for Sm–Nd isochron dating. Crossed nicols.

b and c. Outcrop (no. 142, see Table 5 in electronic supplement) of basaltic pillow-lavas and intercalated red pelagic limestones containing globotruncanids. Note the radial crack filled with limestones in b.

d. Thin section photomicrograph of *Contusotruncana* (anc. *Rosita*) *patelliformis* (Gandolfi, 1955) in pelagic limestone (sample K142s) from the locality in (b), dating the limestones to the Early Campanian. Fossil determination courtesy of M. Caron (Fribourg).

e. Late Cretaceous–Early Paleogene (?) lithic sandstone (sample K144) containing reworked volcanic material from the North Kozara magmatics of both mafic and felsic affinity. D = dolerite clasts with ophitic textures, G = coarse-grained clasts with granophyric texture.

f. Late Cretaceous–Early Paleogene lithic sandstone (sample K144) containing reworked shallow-water benthic foraminifera of the species *Orbitoides gruenbachensis* Papp and Küpper, indicative of Maastrichtian age.

Our paper presents new biostratigraphic, geochronological and geochemical evidence for Late Cretaceous intra-oceanic magmatism within the Sava Zone. These results constrain the earliest possible age for the closure of the Vardar Ocean to the latest Cretaceous. This supports the assumption of Karamata et al. (2000, 2005) that a remnant or a "marginal basin" of the Vardar Ocean stayed open until the Campanian. Our results are also in line with Pamić (1993a, 2002), who interpreted the Sava Zone as a suture that formed during the collision of the Internal Dinarides with Tisza during the Paleogene.

2. Regional geological setting

Outcrops of pre-Neogene rocks in the study area are restricted to isolated inselbergs separated by Neogene fill (Fig. 2). Pre-Neogene rocks cropping out in the Papuk–Psunj inselberg belong to the Tisza Mega-Unit. This is characterised by a pre-Mesozoic basement that experienced a pre-Variscan and Variscan metamorphic overprint (Balen et al., 2006, and references therein), and an autochthonous Permo-Mesozoic, non-metamorphic cover. By contrast, the westerly and southerly adjacent inselbergs of Moslavačka Gora, Požeška Gora, Prosara and Motajica all underwent middle or Late Cretaceous metamorphism. In Moslavačka Gora olivine gabbros were intruded in the late Early Cretaceous (c. 110 Ma, Balen et al., 2003), followed by Late Cretaceous LP-HT (Abukuma-type) metamorphism. This event was accompanied by the formation of migmatites and granites that yielded electron-microprobe-based monazite ages around 80 Ma (Starijaš et al., 2004, 2006). ^{40}Ar–^{39}Ar ages obtained on hornblende (81–83 Ma) and white mica (74 Ma) document cooling from peak metamorphic conditions between 83 and 74 Ma (Balen et al., 2001).

The northern part of Požeška Gora exposes a bimodal igneous rock suite including (gabbro-) dolerites, pillow basalts, basic and acidic tuffs and volcaniclastics, as well as alkali-feldspar rhyolites and subordinate granites (Pamić and Šparica 1983; Belak et al., 1998). The basalts and tuffs are intercalated with red, pelagic limestones that yielded Late Campanian to Early Maastrichtian globotruncanids (Pamić and Šparica 1983). Dolerite dikes intruded both acidic rocks and Late Cretaceous sediments (Belak et al., 1998). Rhyolites and cogenetic granites have a Rb–Sr age of 71.5±2.8 Ma (Pamić et al., 1988), whereas K–Ar ages of the dolerites range between 66 and 68 Ma (Pamić, 1993b). In the south of Požeška Gora, greenschist-facies phyllites predominate. K–Ar whole rock ages obtained on muscovite-rich phyllites yielded an age of ca. 49 Ma (Pamić et al., 1988), which may reflect cooling from earlier peak metamorphic conditions. Due to poor outcrop conditions, the structural relationships between the Late Cretaceous bimodal volcanics and the greenschist-facies metamorphics are presently unknown (see Šparica et al., 1980).

The inselberg of Motajica (Fig. 2) is characterised by a Late Cretaceous, mostly siliciclastic succession that underwent Barrovian-type metamorphism (Pamić and Prohić, 1989; Pamić et al., 1992) and is comparable to the metamorphic series found in Požeška Gora. Electron-microprobe-based analysis of monazites in lower amphibolite-grade metapelites from Motajica yielded an age of 63±9 Ma for this metamorphic event (Krenn et al., 2008).

The inselberg of Prosara exposes a lower tectonic unit in the S and an upper tectonic unit in the N. These units are separated by a N-dipping thrust associated with a top-S shear sense. The lower unit consists of a non-metamorphic succession of sandstones and shales of most likely Paleogene age (Šparica et al., 1984; Jovanović and Magaš, 1986). The higher unit comprises, from bottom to top, a greenschist-facies succession of mylonitic metarhyolites, prasinites, followed by metasandstones, phyllites and subordinate calcite marbles. Palynomorph studies performed on the phyllites suggested a Maastrichtian protolith age (Šparica et al., 1984; Jovanović and Magaš, 1986). Metarhyolites and phyllites are intruded by meter-scale pegmatite dykes and decametric bodies of coarse-grained, leucocratic alkali-feldspar granites. While the dikes are mostly boudinaged, the larger intrusions acquired a schistosity together with their host rock. Thin-section analyses suggest that the schistosity formed in a solid state. These observations suggest that the fabric-forming event occurred after the intrusion of the leucocratic magmatics.

3. Geology and petrography of the Kozara Mountains

The Kozara Mountains (Fig. 3) form a WNW–ESE-trending massif at the southwestern margin of the Pannonian Basin. The outline of this massif follows the general strike of the geological units. Igneous rocks dominate in the northern and southern parts of the Kozara Mountains and are separated from each other by a belt of Eocene turbiditic sandstones (Fig. 3). From south to north, across strike, or in cross-section from bottom to top (Fig. 4), the following geological units can be distinguished.

3.1. South Kozara

The lowermost unit exposed consists of Bathonian to Valanginian-age radiolarites (Djerić and Vishnevskaya, 2006; Djerić et al., 2007), which belong to the East Bosnian–Durmitor unit (Schmid et al., 2008). The Durmitor unit tectonically overlies the Pre-Karst unit, which is characterised by a Late Paleozoic to Late Cretaceous sedimentary succession. The radiolarites of the Durmitor unit are tectonically overlain by an ophiolitic mélange that consists predominantly of disrupted lithic sandstones and shales. Numerous extra-formational blocks of mafics, ultramafics and Late Triassic shallow-water limestones and dolomites occur within the mélange. The Triassic olistoliths are up to several km across and often form the highest mountains (Lisina 978 m, Fig. 3). The lithic sandstones are moderately to poorly sorted and both texturally and compositionally immature. The most frequent detrital components are euhedral, often embayed quartz grains of volcanic origin, plagioclase, white mica and basalt fragments. The shales typically exhibit an intense, closely spaced cleavage. The exact age of formation of the ophiolitic mélange in Kozara and elsewhere in the Dinarides is still poorly constrained. Near Zagreb, the shaly matrix of the ophiolitic mélange was dated by palynomorphs, yielding ages from Hettangian to Late Bajocian (Babić et al., 2002). In our opinion, the Bajocian age indicates the maximum age of the mélange formation (see below).

In South Kozara, an ultramafic to mafic succession tectonically overlies the ophiolitic mélange. In contrast to other ophiolite exposures in the Dinarides, no metamorphic sole has yet been found here. The ultramafics are often serpentinised lherzolites (Djerković et al., 1975; Mojićević et al., 1976). The mafics include gabbros and dolerites. Volumetrically subordinate dolerites occur usually as dikes cutting the gabbros. No doleritic sheeted dike complex was recognised; basalts are totally absent. Gabbros show both isotropic, cumulate and, rarely, pegmatitic textures. The cumulates are olivine bearing and coarse grained with ophitic to subophitic textures. Olivine is partly transformed into iddingsite (made up of cryptocrystalline chlorite and goethite). Plagioclase and clinopyroxene are fresh in some samples (Plate Ia; sample K135). Clinopyroxene forms large, poikilitic grains. Subordinately, albite-rich felsic intrusives and dikes occur. The latter cut both gabbros and dolerites, show granophyric textures and contain zoned plagioclase.

The mélange together with the ultramafics and mafics are unconformably overlain by reddish pelagic marly limestones and clast-supported micro-conglomerates with pebbles of pelagic limestone (Fig. 3). The age of the pebbles ranges from latest Albian to Coniacian–Santonian, as indicated by different species of planktonic foraminifera (M. Caron pers. comm. 2006). The matrix, and hence the conglomerate formation, is thus most likely of Campanian age or younger.

Higher up in the section, the lithologies so far described are unconformably overlain by an Upper Paleocene to Eocene succession starting with often bioclastic shallow-water limestones (column "S

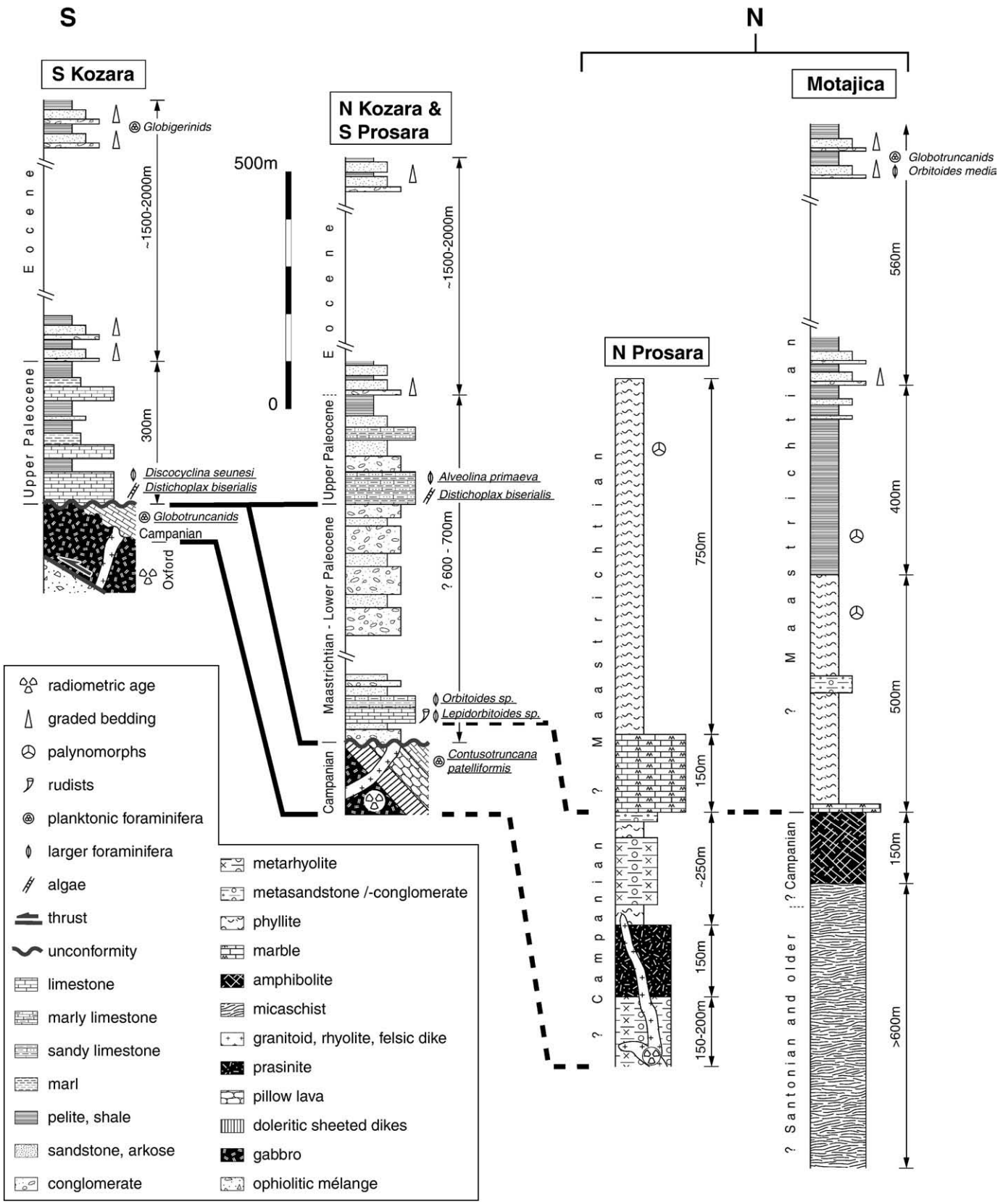

Fig. 5. Tectono-stratigraphic correlation of the North Bosnian inselbergs (south of the Sava River, see Fig. 2). Bold black lines mark correlated stratigraphic intervals and unconformities. Fossils identified in this study are underlined. Correlations between the exposures in South and North Kozara rely on both litho- and biostratigraphy, whereas further correlations with Prosara and Motajica are largely based on lithostratigraphy. For simplicity, the (Late Oligocene) Motajica granitoid (shown in Fig. 2) is omitted in the corresponding stratigraphic column.

Kozara" in Fig. 5). The limestones are packstones, grainstones and rudstones, containing *Discocyclina*, red algae (*Distichoplax biserialis*), coral fragments, alveolinids, and rare globigerinids (Jovanović and Magaš, 1986; M. Caron pers. comm., 2006). Up-section, they grade into marls and shales (Fig. 5). Still higher up follows a succession of thick-bedded siliciclastic turbiditic sandstones (arkoses, lithic arenites, lithic sandstones) and subordinate pelites. The basal part of this succession includes reworked bioclasts. The detrital components are mostly quartz (often embayed quartz of volcanic origin), plagioclase, microcline, white mica and biotite. Rock fragments are mostly basalts, granophyres and metamorphics of both low and high grade. Bed thickness ranges from about 10 cm to 1 m. Individual beds are commonly graded. Globigerinids within hemipelagic intercalations (Jelaska, 1981), as well as benthic foraminiferal assemblages (Šparica et al., 1984), constrain the minimum age of this succession to the middle Eocene.

3.2. North Kozara

The turbiditic sandstone succession of South Kozara dips N and is overlain by the igneous succession of North Kozara, separated by a major thrust (Fig. 4). The igneous succession comprises gabbros, dolerites, doleritic sheeted dikes, basalts and subordinate peraluminous (Shand, 1947) felsic dikes and extrusives (Figs. 3, 4), and substantially differs from that of South Kozara. Ultramafics do not crop out: the structurally lowest exposed levels are gabbros, and hence there is no direct proof that the latter are underlain by ultramafics. The gabbros are coarse to very coarse grained with isotropic textures. The main mineral phases are plagioclase and brown and green amphibole. Green amphibole is formed by replacement (uralitisation) of primary clinopyroxene. Common accessory minerals are biotite, apatite, zircon and Fe–Ti-oxides.

The dolerites are subophitic with idiomorphic plagioclase laths, clinopyroxene, brown and green hornblende. Biotite has formed at the expense of brown hornblende. Accessories are zircon, apatite and Fe–Ti-oxides. Plagioclase is often zoned.

The basalts are usually phaneritic and typically show intersertal textures formed by elongated laths of idiomorphic plagioclase. Porphyritic varieties with idiomorphic olivine phenocrysts are also found. The top of the mafic igneous succession consists of pillow lavas, containing amygdules with calcite. The pillow lavas are intercalated with red pelagic limestones of Scaglia facies that are also found as inter-pillow sediment and along radial cracks in the pillows (Plate Ib and Ic). This indicates that the extrusion of the pillow lavas and the sedimentation of the pelagic limestones were contemporaneous. The occurrence of *Contusotruncana* (anc. *Rosita*) *patelliformis* (Gandolfi) constrains the age of the pelagic limestones and, indirectly, the pillow basalts, to the Early Campanian (Plate Id, determination by M. Caron). Karamata et al. (2000, 2005) suggested a Late Campanian to Early Maastrichtian for these same limestones.

The mafics are often intruded by felsic dikes on the outcrop scale. On the map scale, rhyolites are found in numerous locations (Fig. 3). Composite dikes of mafic amphibole-bearing segments in diffuse contact with granophyric segments are occasionally found, suggesting simultaneous mafic and felsic intrusion. Rhyolites are mostly altered, fine-grained, banded and commonly of aphyric texture.

The map view alignment of the gabbros (in the north), dolerites and pillow basalts, including their cover of pelagic limestones (in the south) suggests that the igneous succession is tilted towards the S and even overturned in proximity to the north-dipping thrust fault (Fig. 4). This is corroborated by the following observations: (a) The beds of the pelagic limestones, intercalated with the pillow lavas, dip to the S or are even overturned and then topographically overlain by igneous rocks and (b) the chilled margins within the originally subvertical doleritic sheeted dike complex dip to the NNE- to NE (upper stereoplot in Fig. 3).

Arkoses, lithic sandstones, conglomerates and shallow-water limestones unconformably overlie the igneous rocks of North Kozara. The shallow-water limestones contain abundant rudist fragments and benthic foraminifera indicating a Maastrichtian age (Fig. 3, column "N Kozara & S Prosara" in Fig. 5). Lithic sandstones, overlying the shallow water limestones, contain reworked benthic foraminifera of Maastrichtian age and abundant fragments of basalt and granophyre (Plate Ie and If, Plates II and III in electronic supplement). Quartz, plagioclase and detrital white mica are also very common. Thick beds of poorly sorted conglomerates with well-rounded boulders/clasts, ranging from a few cm up to several dm in diameter, consist of basalts, dolerites and granite clasts. Metamorphic rocks are absent. Up-section, the average clast size of the conglomerates decreases. Bioclastic limestones with alveolinids, indicating a Late Paleocene (Thanetian) age (Fig. 5, Plate IV in electronic supplement) are intercalated.

4. Geochemistry and age of the Kozara Mountains igneous rocks

A geochemical comparison of the two tectonically separated igneous complexes exposed in the South and North Kozara Mountains, respectively, is precluded by the fact that both igneous complexes

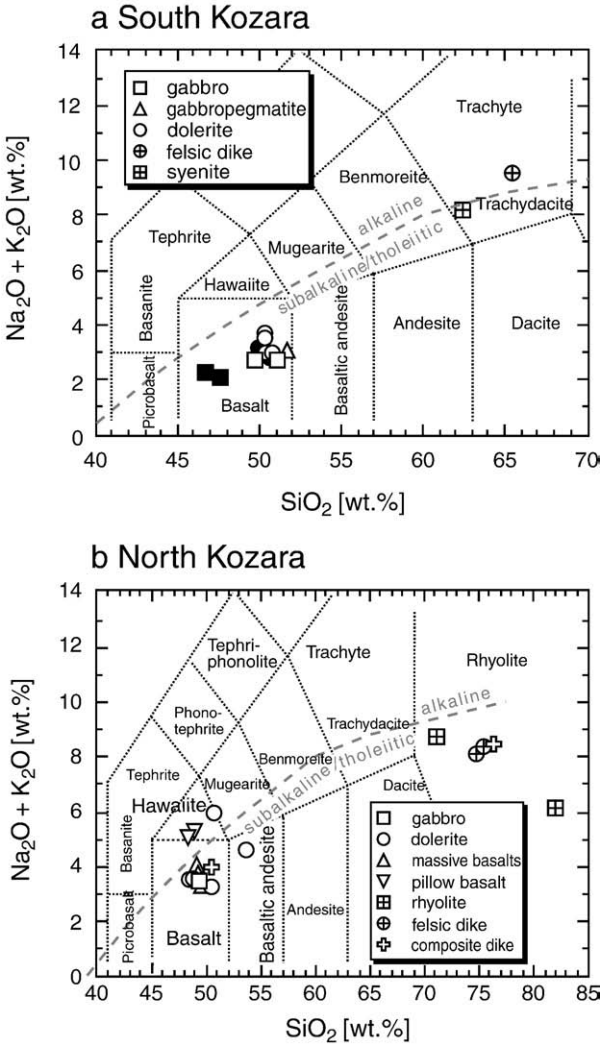

Fig. 6. TAS diagrams (after Le Bas et al., 1986) of (a) South and (b) North Kozara igneous rocks. Open symbols are samples from this study; black symbols in (a) are samples from Lugović et al. (1991).

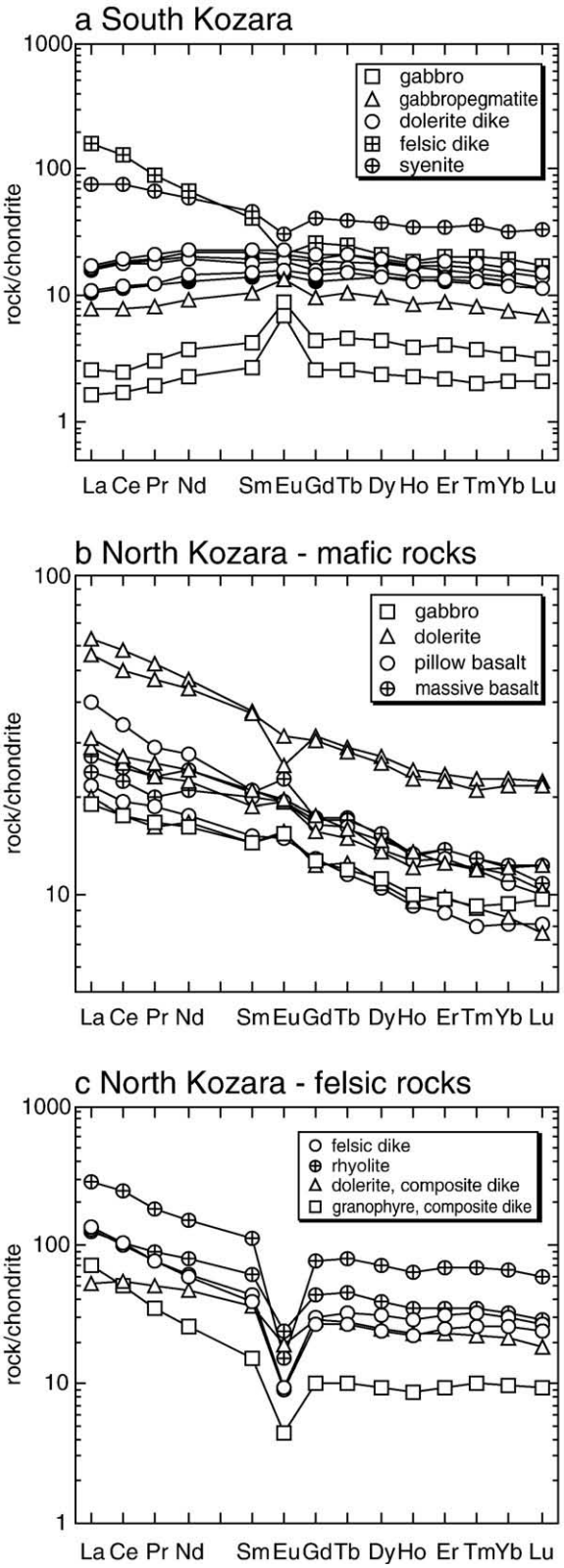

Fig. 7. Rare earth element concentrations normalised over chondrite composition. a: South Kozara, b: North Kozara mafic rocks, c: North Kozara felsic rocks. Chondrite normalisation is according to Boynton (1984). Open symbols are from this study; filled symbols are from Lugović et al. (1991).

represent incomplete ophiolitic successions, each comprising different crustal levels. The absence of extrusive rocks in South Kozara makes it impossible to directly compare the South Kozara rocks with the unfractionated basaltic rocks from North Kozara. Hence, our interpretation of the tectonic setting of the South and North Kozara igneous successions does not solely rely on the analysis of geochemical discrimination diagrams, but, in addition, on isotopic evidence as well as on the field geological constraints given above. 26 whole-rock samples were analysed for major and trace elements (Table 1). The majority of the analysed samples (23) yielded loss-on-ignition (LOI) values of <4 wt.% indicating that their degree of alteration is low to moderate. LOI is generally higher for the North Kozara samples (up to 9 wt.%) and apparently in line with the occurrence of hydrous mineral phases.

4.1. South Kozara

4.1.1. Major and trace element characteristics

In the TAS-diagram (total alkali (Na_2O+K_2O) vs. SiO_2 ratio; Le Bas et al., 1986), samples from South Kozara almost exclusively plot in the field of subalkaline/tholeiitic basalts (Fig. 6a). Gabbros from South Kozara are low in TiO_2 (<0.3%) and K_2O (<0.4%) with Mg# between 69 and 74 (Mg# = 100 * molar $MgO/(MgO+FeO_{total})$). Dolerites show slightly higher contents of TiO_2 (up to 1.6%) and Mg# between 57 and 62. Mg# and Ti-content are negatively correlated. Concentrations

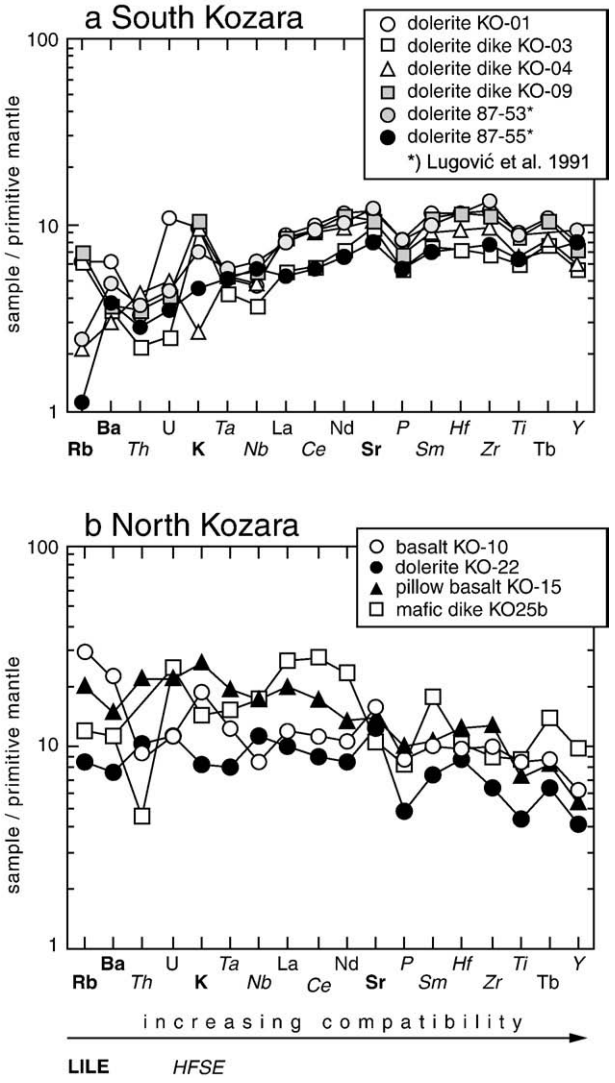

Fig. 8. Primitive mantle-normalised multi-element diagrams of non-cumulate South Kozara mafic rocks (a) and North Kozara mafic rocks (b). Normalisation values are after Hofmann (1988).

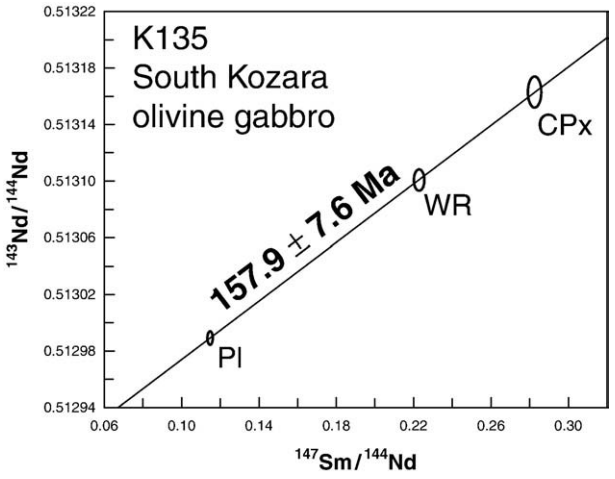

Fig. 9. Sm–Nd-isochron plot of an olivine-bearing cumulate gabbro from South Kozara. The three data points (Pl = Plagioclase, WR = whole-rock, CPx = clinopyroxene) fit onto an isochron with an age of 158 ± 8 Ma (MSWD 0.0109). The initial $^{143}Nd/^{144}Nd$ value is 0.512871 ± 9 (see Table 2). See Figs. 4 and 12 for sample locality.

of compatible elements, like Ni and Cr, correlate positively with Mg#. Chondrite-normalised REE concentration diagrams of samples from South Kozara (particularly gabbros) reveal essentially flat REE patterns (Fig. 7a), with a slight depletion of LREE. The felsic dikes and intrusives show enrichment of LREE over HREE. Positive Eu-anomalies in the gabbros are attributed to fractionation of Eu^{2+} into plagioclase, a main constituent phase in the gabbros. Primitive mantle-normalised multi-element diagrams of non-cumulate mafic samples show gently positive slopes and unpronounced depletions in P and Ti (Fig. 8a).

4.1.2. Sm–Nd dating, Sr and Nd isotopes

A well-preserved, coarse-grained olivine gabbro from South Kozara, with fresh plagioclase and clinopyroxene, was chosen for dating (sample K135). A whole-rock powder, clinopyroxene and plagioclase were used for dating. The data points fit onto an isochron, yielding an age of 158 ± 8 Ma (MSWD 0.0109). The initial $^{143}Nd/^{144}Nd$ value is 0.512871 ± 9 (Fig. 9 and Table 2).

Sr- and Nd-isotopic values were also analysed on a whole-rock powder of the same sample, yielding an $^{87}Sr/^{86}Sr$-ratio of 0.702703 and a $^{143}Nd/^{144}Nd$-ratio of 0.513067. Its initial isotopic values, calculated for an age of 160 Ma, are +8.6 for εNd(T) and 0.70264 for $^{87}Sr/^{86}Sr$, respectively (Fig. 10 and Table 3). The sample plots in the MORB field.

4.2. North Kozara

4.2.1. Major and trace element characteristics

In the TAS-diagram (Le Bas et al., 1986), samples from North Kozara plot as subalkaline/tholeiitic basalts, basaltic andesites, hawaiites and rhyolites, and they show a bimodal distribution (Fig. 6b). Mg# of all samples (except felsic dikes or intrusives) are between 40 and 66 (Table 1), i.e. they are generally more evolved than comparable samples from South Kozara. The basalts and basaltic andesites reveal K_2O contents between 0.25 and 1.14 wt.%. Based on this, they can be classified as low- to medium-K tholeiites (Gill, 1981).

Chondrite-normalised REE patterns of samples from North Kozara show strong enrichment of LREE over HREE (Fig. 7b and c). None of the essentially flat REE patterns that characterise the South Kozara mafic igneous rocks are encountered here. The REE slopes of both mafic and felsic samples are essentially parallel. A primitive mantle-normalised multi-element diagram is shown for four mafic igneous rocks (Fig. 8b). This shows no significant depletion of HFSE (particularly Ta, Nb, P, Zr and Ti) over LILE (Rb, Ba and Sr).

4.2.2. Sr and Nd isotopes

The $^{143}Nd/^{144}Nd$-ratios of the North Kozara samples are similar, varying between 0.512844 and 0.512945 (Table 3). By contrast, the $^{87}Sr/^{86}Sr$-ratios of the same samples exhibit a relatively large spread between 0.703531 and 0.706224. The initial isotopic values for 80 Ma (see below) are +4.4 to +6.3 for εNd(T) and 0.70346 to 0.70507 for $^{87}Sr/^{86}Sr$, respectively (Fig. 10). The εNd(T) values and initial $^{87}Sr/^{86}Sr$-ratios from North Kozara plot at the intersection between the MORB, island arc and ocean island basalt fields. Two "outliers" with the highest $^{87}Sr/^{86}Sr$-ratios (samples K142 and K147b) are an altered pillow basalt with calcite-filled amygdules and a veined dolerite, respectively; they also yielded LOI values of up to 9% (Table 1).

4.2.3. U–Pb dating

Three igneous rock samples have been selected for high accuracy isotope-dilution thermal ionisation mass spectrometry (ID-TIMS) dating using zircon single crystals. Two samples (a dolerite and a rhyolite, samples K149 and UK06-34, respectively) are from North Kozara, a third sample is from Prosara Mountain (an alkali-feldspar granite, sample UK04-4) located still further north (Figs. 2 & 4). The results are presented in Fig. 11 and Table 4. The three dated samples (K149, UK06-34 and UK04-02) yielded weighted mean $^{206}Pb/^{238}U$ ages of 81.4 ± 0.11 Ma, 81.6 ± 0.12 Ma and 82.68 ± 0.13 Ma, respectively.

5. Discussion

5.1. Tectonic interpretation of the geochemical and isotopic data

From a tectonic point of view, the ultramafic and igneous succession of South Kozara represents the northwesternmost occurrences of the Western Vardar Ophiolitic Unit. This is evident from the overall geological framework and is further corroborated by our new geochronological data.

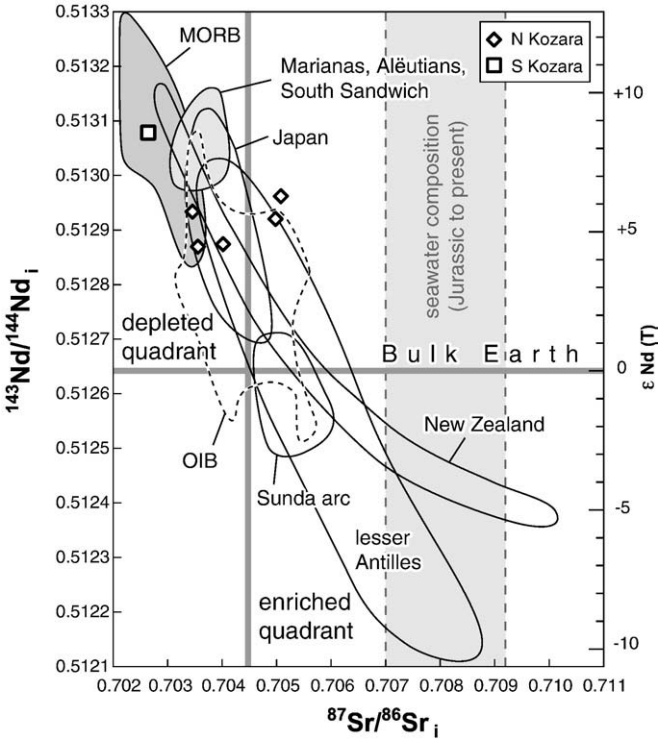

Fig. 10. Initial Nd- and Sr-isotopic ratios of selected North and South Kozara mafics in comparison to various basaltic rocks from different oceanic environments. The samples with elevated $^{87}Sr/^{86}Sr$ values are likely affected by syn- or postmagmatic alteration in contact with seawater, the average composition of which is shown by light-grey shading. The OIB field is after Hofmann (1997), all other fields are from Murphy (2007).

Table 1
Whole rock chemical analyses of igneous rocks from South and North Kozara

South Kozara									
Sample rock remark	K135 ol-gabbro cumulate	KO-05 gabbro cumulate	KO-07 gabbro pegm	KO-01 dolerite massive	KO-03 dolerite dike	KO-09 dolerite dike	KO-04 dolerite dike	KO-08 TD dike	KO-H alb.sy intr
SiO_2	49.09	49.70	50.13	49.08	49.69	49.48	49.25	64.21	60.46
TiO_2	0.25	0.31	0.70	1.64	1.09	1.52	1.22	0.89	1.28
Al_2O_3	19.62	17.62	14.70	15.33	15.48	15.59	16.15	18.99	15.19
$Fe_2O_{3\ total}$	6.46	5.88	7.52	10.60	9.08	10.37	9.08	2.00	6.17
MnO	0.11	0.09	0.12	0.17	0.15	0.17	0.15	0.02	0.09
MgO	9.08	8.77	9.04	7.25	8.41	7.41	7.95	1.67	1.74
CaO	11.42	12.29	11.88	9.85	10.92	10.17	10.91	0.82	3.54
Na_2O	2.56	2.61	2.60	3.29	2.60	3.16	2.81	9.40	6.19
K_2O	0.13	0.07	0.37	0.30	0.30	0.33	0.08	0.00	1.78
P_2O_5	0.03	0.01	0.04	0.17	0.12	0.14	0.14	0.18	0.49
LOI	1.51	2.02	2.24	1.29	1.32	1.30	1.51	1.20	3.10
Total	100.25	99.37	99.34	98.97	99.16	99.64	99.25	99.38	100.03
Mg#	73.5	74.7	70.4	57.5	64.7	58.6	63.4	62.3	35.8
Rb	1.8	1.6	5.3	3.3	3.4	3.8	1.1	1.0	22
Ba	27	13	33	38	21	22	18	20	158
Th	0.02	0.05	0.20	0.26	0.18	0.27	0.34	15.0	8.3
U	<0.01	0.01	0.06	0.22	0.05	0.08	0.10	2.14	2.80
Ta	0.25	0.01	0.06	0.18	0.15	0.19	0.19	1.39	1.00
Nb	0.22	0.29	1.0	2.8	2.3	3.5	3.0	18	13
Pb	<1	<5	<5	<5	<5	<5	<5	6.74	0.70
Sr	189	222	192	215	173	190	193	49	137
Zr	7	12	34	116	66	109	94	284	428
Hf	0.23	0.45	1.04	3.11	1.95	3.08	2.51	8.15	11.8
Y	5	7	15	31	23	28	24	34	72
V	70	104	182	241	212	226	194	98	128
Cr	371	407	153	220	353	260	260	82	7
Ni	178	113	107	57	101	57	93	35	4
Co	57	34	37	38	39	38	38	8	11
Zn	40	32	37	73	72	80	62	<30	52
La	0.50	0.79	2.4	5.4	3.4	5.1	5.2	50.3	23.7
Ce	1.4	2.0	6.3	15.8	9.4	14.9	14.4	103.9	61.3
Pr	0.24	0.37	1.0	2.5	1.5	2.4	2.2	10.8	8.1
Nd	1.34	2.26	5.54	13.7	8.66	13.2	11.4	39.7	35.4
Sm	0.51	0.82	2.03	4.39	2.95	4.23	3.43	7.88	9.00
Eu	0.508	0.657	0.987	1.66	1.16	1.57	1.38	1.57	2.21
Gd	0.68	1.1	2.5	5.4	3.7	5.0	4.1	6.7	10.7
Tb	0.12	0.22	0.49	1.02	0.72	0.99	0.77	1.19	1.87
Dy	0.77	1.4	3.1	6.2	4.4	5.9	4.8	6.7	11.8
Ho	0.16	0.28	0.62	1.28	0.92	1.22	0.99	1.34	2.46
Er	0.46	0.85	1.83	3.93	2.77	3.65	2.98	4.29	7.42
Tm	0.065	0.123	0.264	0.574	0.412	0.533	0.447	0.667	1.16
Yb	0.44	0.73	1.56	3.49	2.52	3.23	2.70	4.04	6.76
Lu	0.069	0.101	0.228	0.482	0.360	0.451	0.370	0.562	1.08

North Kozara									
Sample rock remark	K150 a-gabbro isotropic	K146* dolerite massive	K147b K-TB a-opx-	K149b a-BA massive	KO-22 dolerite massive	KO-24 dolerite pegm	KO-10 Basalt aphyric	KO-23 basalt aphyric	KO-12 basalt porphyric
SiO_2	48.25	46.51	47.27	53.01	49.67	47.19	48.05	48.97	48.09
TiO_2	1.36	1.45	2.43	2.05	0.81	2.45	1.55	2.21	1.70
Al_2O_3	16.93	18.43	13.61	14.67	16.18	16.26	15.20	14.94	17.30
$Fe_2O_{3\ total}$	9.32	9.43	12.78	11.30	8.09	10.27	10.32	13.31	10.08
MnO	0.14	0.22	0.22	0.20	0.21	0.14	0.16	0.13	0.15
MgO	6.83	5.95	4.39	4.90	8.02	6.75	6.90	5.66	5.11
CaO	11.25	10.10	6.71	8.04	12.01	10.50	11.49	10.10	11.17
Na_2O	3.04	2.95	3.49	3.68	2.91	3.23	2.96	3.79	2.82
K_2O	0.40	0.42	2.07	0.85	0.26	0.24	0.58	0.25	0.43
P_2O_5	0.11	0.18	0.32	0.26	0.10	0.17	0.18	0.26	0.21
LOI	1.67	3.37	7.18	1.26	1.31	1.82	2.54	0.25	1.62
Total	99.30	99.00	100.47	100.22	99.57	99.02	99.93	99.87	98.68
Mg#	59.2	55.5	40.5	46.2	66.3	56.6	57.0	45.7	50.1
Rb	4.7	11	56	18	4.6	3.5	16	2.7	11
Ba	70	113	326	189	46	47	133	46	96
Th	0.57	1.00	2.08	4.17	0.86	1.95	0.71	0.61	0.51
U	0.21	0.35	0.75	1.36	0.23	0.48	0.23	0.30	0.16
Ta	0.60	0.64	1.10	2.36	0.28	0.67	0.44	0.69	0.51
Nb	5.5	6.6	14	17	6.9	12	5.3	12	7.8
Pb	<1	2.2	8.1	3.2	<5	<5	<5	<5	<5
Sr	238	266	149	209	226	288	288	226	266
Zr	73	100	220	223	62	111	99	139	92
Hf	1.95	2.49	5.16	5.40	2.36	3.24	2.60	4.10	2.62
Y	20	29	47	50	17	21	24	34	24

(continued on next page)

Table 1 (*continued*)

North Kozara									
Sample rock remark	K150 a-gabbro isotropic	K146* dolerite massive	K147b K-TB a-opx-	K149b a-BA massive	KO-22 dolerite massive	KO-24 dolerite pegm	KO-10 Basalt aphyric	KO-23 basalt aphyric	KO-12 basalt porphyric
V	203	212	227	252	158	261	228	281	207
Cr	269	282	34	82	241	62	270	73	140
Ni	71	63	17	28	74	76	64	63	21
Co	43	46	34	84	33	35		37	32
Zn	38	82	165	101	39	34	79	33	74
La	6.0	9.6	17.3	19.5	6.2	8.9	7.5	13.5	8.3
Ce	14.3	21.9	40.8	46.8	14.4	20.9	18.3	31.0	20.2
Pr	2.07	3.14	5.72	6.41	1.99	2.83	2.48	4.43	2.86
Nd	9.77	14.76	26.28	28.28	10.11	13.57	12.80	22.15	14.74
Sm	2.84	4.10	7.19	7.33	2.82	3.69	3.90	6.16	4.05
Eu	2.84	4.10	7.19	7.33	2.82	3.69	3.90	6.16	1.68
Gd	3.32	4.62	7.90	8.10	3.23	4.08	4.47	6.71	4.52
Tb	0.57	0.76	1.32	1.38	0.59	0.72	0.81	1.23	0.83
Dy	3.58	4.74	8.25	8.58	3.48	4.36	4.94	7.28	4.91
Ho	0.72	0.97	1.65	1.75	0.69	0.88	0.97	1.48	0.95
Er	2.03	2.66	4.74	4.95	2.07	2.66	2.91	4.45	2.93
Tm	0.299	0.390	0.689	0.740	0.295	0.396	0.420	0.634	0.423
Yb	1.98	2.53	4.57	4.81	1.78	2.42	2.58	3.84	2.55
Lu	0.313	0.396	0.707	0.732	0.246	0.333	0.400	0.526	0.351

Sample rock remark	KO-15 basalt pillow	K142 basalt pillow	KO-14 rhyolite dike	KO-16 rhyolite dike	KO-17 rhyolite massive	KO-20 rhyolite massive	KO-25c Granoph cmp.dk	KO-25b a-dol cmp.dk
SiO_2	45.15	44.97	73.98	73.85	68.53	80.91	75.30	49.98
TiO_2	1.29	1.32	0.28	0.22	0.59	0.16	0.11	1.58
Al_2O_3	15.91	14.26	13.57	13.06	13.81	9.46	13.07	14.92
$Fe_2O_{3\ total}$	9.31	9.00	1.85	1.80	4.09	1.48	0.86	11.68
MnO	0.19	0.19	0.01	0.04	0.07	0.01	0.01	0.13
MgO	6.22	5.65	0.32	0.38	0.53	0.42	0.16	6.87
CaO	10.05	11.57	0.76	0.33	0.21	0.10	0.84	9.91
Na_2O	3.87	3.80	5.23	3.15	1.26	0.26	3.99	3.47
K_2O	0.80	1.14	2.82	5.08	7.21	5.77	4.35	0.45
P_2O_5	0.21	0.14	0.05	0.05	0.15	0.03	0.01	0.17
LOI	6.18	8.72	0.58	2.02	2.56	1.46	0.34	0.76
Total	99.18	100.77	99.45	99.97	99.01	100.06	99.05	99.92
Mg#	57.0	55.4	25.5	29.5	20.4	36.0	26.9	53.8
Rb	11	19	60	119	125	170	151	6.5
Ba	89	165	258	551	867	294	222	68
Th	1.76	0.61	18.9	16.4	11.3	20.6	28.6	0.37
U	0.44	0.45	6.09	7.37	3.94	2.52	2.64	0.51
Ta	0.69	0.58	1.68	1.67	1.70	4.52	1.51	0.54
Nb	11	7.6	19	18	25	57	8.6	11
Pb	<5	8.2	<5	8.0	16.1	8.2	<5	<5
Sr	255	245	82	59	36	18	49	198
Zr	124	86	321	256	454	972	108	86
Hf	3.38	2.11	9.75	8.25	11.7	26.2	5.42	2.78
Y	21	19	41	52	58	104	16	39
V	167	186	4	3	8	2	7	252
Cr	313	278	<20	<20	<20	20	20	156
Ni	139	77	<20	<20	<20	<20	42	47
Co	44	33	1	2	4	<1	3	39
Zn	72	73	<30	42	1980	75	<30	33
La	12.4	6.8	41.2	40.2	38.0	89.0	22.4	16.6
Ce	27.6	15.9	84.6	81.3	85.1	194.6	41.8	44.9
Pr	3.55	2.29	9.49	9.32	10.80	22.58	4.27	6.24
Nd	16.40	10.70	36.05	36.89	47.63	91.37	15.36	27.93
Sm	4.15	3.00	7.48	8.38	11.90	21.49	2.93	6.96
Eu	1.43	1.10	0.654	0.691	1.79	1.12	0.324	6.96
Gd	4.28	3.35	6.83	7.91	11.22	20.10	2.66	7.40
Tb	0.77	0.55	1.27	1.55	2.12	3.84	0.49	1.32
Dy	4.44	3.36	7.74	9.85	12.50	22.91	2.97	7.99
Ho	0.91	0.66	1.60	2.10	2.46	4.58	0.62	1.63
Er	2.72	1.84	5.28	6.63	7.29	14.38	2.01	4.92
Tm	0.387	0.260	0.849	1.047	1.124	2.252	0.324	0.729
Yb	2.28	1.70	5.45	6.33	6.73	13.69	2.07	4.40
Lu	0.321	0.262	0.777	0.851	0.925	1.884	0.302	0.603

Major element oxides in wt.%, trace elements in ppm. LOI=loss on ignition. Mg#=100∗molar MgO/(MgO+FeO_{total}). Rock abbreviations: TD=trachydacite; alb.sy=albite syenite; K-TB=potassic trachybasalt; BA=basaltic andesite; pegm=pegmatitic rocks; granoph=granophyre; dol.=dolerite. a-, opx-=igneous amphibole and orthopyroxene bearing assemblage. dol=dolerite; cmp.dk=composite dike (of granophyre and amphibole dolerite).

*Sample was a c. 50 cm diameter pebble retrieved from conglomerates overlying the igneous succession.

Table 2
Sm–Nd-isotopic data of sample K135 from South Kozara

Sample	Nd [ppm]	Sm [ppm]	$^{147}Sm/^{144}Nd$	$^{143}Nd/^{144}Nd$	2Sd (m)
K135WR	2.610	0.962	0.2228	0.513101	0.000006
K135 CPx	5.580	2.607	0.2825	0.513163	0.000009
K135 Pl	0.767	0.146	0.1147	0.512989	0.000004

Given Sm and Nd concentrations were detected by isotope dilution. For calculating the isochron age an error of 1% at the $^{147}Sm/^{144}Nd$ ratio was assumed. WR = whole rock, Cpx = Clinopyroxene, Pl = Plagioclase.

The bimodal igneous succession of North Kozara tectonically overlies the Western Vardar Ophiolitic Unit and — according to the available geological and geochronological data — is of different age. However, the available geochemical and isotopic data do not allow the North Kozara igneous succession to be assigned to any particular geodynamic setting. The bimodal nature of volcanism is not distinctive of a mid-ocean ridge (MOR), ocean island (OI) or island-arc (IA) setting. The enrichment of LREE over HREE at least opposes a normal mid-ocean ridge (N-MOR) origin (Schilling et al., 1983). The negative and mutually parallel REE slopes of both mafic and felsic rocks suggest that they were derived from the same magma source. Primitive mantle-normalised multi-element diagrams do not show depletion of HFSE (particularly Nb, Ta and Ti) over LILE. There is no spiked pattern, which is typical of subduction-related magmatics (Sun and Stern, 2001; Murphy, 2007). Instead, they are more consistent with an OI origin (Hofmann, 1997; Winter, 2001). The absence of boninitic lavas (Cameron et al., 1979), considered typical of intraoceanic island arcs (Hickey and Frey, 1982; Crawford et al., 1981; Kim and Jacobi, 2002), is another argument against an IA setting.

The $^{143}Nd/^{144}Nd$-ratios of the analysed mafic rocks from North Kozara are uniform and further suggest that the North Kozara magmatics are co-genetic. The larger scatter in $^{87}Sr/^{86}Sr$-ratios with two outliers, on the other hand, is likely to be caused by syn- or post-magmatic alteration. The isotopic ratios are equivocal in terms of attributing the North Kozara magmatics to an IA, OI or MOR setting, as these fields strongly overlap (Fig. 10; Hofmann, 1997). In any case, the isotopic ratios do not suggest that the North Kozara magmatics formed in a continental ("Andean") volcanic arc setting, which typically yields much higher $^{87}Sr/^{86}Sr$- and lower $^{143}Nd/^{144}Nd$-ratios (e.g. Mahlburg Kay et al., 2005). Hence, the pertinent conclusion from a tectonic viewpoint is that it is far more likely that the bimodal igneous succession of North Kozara represents intraoceanic rather than continental magmatism. We take this as evidence that the Adriatic and Europe-derived smaller plates (the Tisza and Dacia Mega-Units) were still separated by a deep basin that was floored by oceanic lithosphere in the Late Cretaceous.

5.2. Growth and demise of Late Cretaceous intraoceanic volcanic islands in the Sava Zone

In spite of the ambivalent geochemical and isotopic data, there is additional geological evidence that favours an interpretation of the Campanian igneous succession documented in the North Kozara and Prosara Mountains (as well as other inselbergs in the Sava Zone) as intraoceanic. Volcanism in North Kozara was present in the Early Campanian in a deep-water environment. At about the same time, the South Kozara ophiolites were unconformably covered by pelagic limestones and microconglomerates that also contain clasts of older pelagic limestones, but no igneous rock debris. This implies that the South Kozara succession did not receive much, if any, detrital input from the time-equivalent volcanic edifice developing in North Kozara. Apart from the structural evidence, this suggests that the two igneous rock massifs must have originally been located at a considerable distance from each other and that they were tectonically juxtaposed later.

Throughout the Campanian, the volcanic build-ups had apparently grown high enough to become exposed above the sea level, as evidenced by the unconformably overlying alluvial conglomerates and sandstones that exclusively rework the underlying igneous succession. As yet, there is no evidence for reworked metamorphic rocks that would indicate a continental source. It is hence conceivable that the formations exposed in the North Kozara and Prosara Mountains became oceanic islands. Intercalations of Maastrichtian and, higher up-section, Paleocene neritic limestones, which may have fringed the volcanic island, constrain the timing of erosion of the volcanic complex. The absence of any intercalated lavas or volcaniclastics within the unconformable cover suggests that volcanic activity was probably confined to the Campanian, in agreement with our radiometric ages.

The South Kozara igneous rocks also possess a similar cover of Paleocene neritic limestones of about the same age. A gradual transition from the Paleocene neritic limestones into an Eocene turbiditic sandstone succession is observed in both South and North Kozara. This suggests that these two units were tectonically juxtaposed earlier, most likely by Maastrichtian-age top-to-the-south thrusting (Fig. 4). This older (Maastrichtian) thrust appears to have been reactivated after the deposition of the turbiditic sandstone succession, i.e. after the middle Eocene. An upper time bracket for the age of this Cenozoic thrust reactivation and displacement along a northerly adjacent thrust in Prosara Mountain is provided by the Neogene sediments of the Pannonian Basin that seal these thrusts. The Paleogene age of this thrusting therefore corresponds to the main phase of nappe stacking that is well known throughout the entire Dinarides (Tari-Kovačić and Mrinjek, 1994).

In summary, the area of the Kozara Mountains documents three phases of compressional tectonics, each separated by one or more unconformities: (1) Late Jurassic obduction, (2) Cretaceous subduction, followed by latest Cretaceous collision, as is evidenced by the juxtaposition of the North Kozara intraoceanic volcanic island with the Western Vardar Ophiolitic Unit and (3) Paleogene (post-Middle Eocene and pre-Miocene) top-to-the-south thrusting (Fig. 4).

5.3. Geodynamic significance of the new radiometric ages

Fig. 12 provides an overview of radiometric ages for ophiolitic lithologies of the northern Balkan Peninsula. The age of the South Kozara gabbro (157.9±7.6 Ma) is among the youngest ages from the

Table 3
Nd- and Sr-isotopic data of selected mafic samples from South and North Kozara

Sample	locality	$^{143}Nd/^{144}Nd$	+/−Sm	$^{87}Sr/^{86}Sr$	+/−Sm	Rb [ppm]	Sr [ppm]	Sm [ppm]	Nd [ppm]	$^{87}Rb/^{86}Sr$	Age [Ma]	Io	$^{147}Sm/^{144}Nd$	e0 Nd (Chur)	Age [Ma]	et $Nd_{(Chur)}$	$T^{Nd}_{(DM)}$ [Ma]
K 135	S Kozara	0.513101	0.000004	0.702703	0.000005	1.7	188	0.96	2.61	0.0261	160	0.70264	0.2228	9.0	160	8.6	
K 142	N Kozara	0.512945	0.000004	0.705330	0.000005	19	245	3	10.7	0.2243	80	0.70507	0.1695	6.0	80	6.3	492
K 146	N Kozara	0.512855	0.000004	0.704150	0.000004	11	266	4.1	14.8	0.1196	80	0.70401	0.1675	4.2	80	4.5	725
K 147b	N Kozara	0.512900	0.000004	0.706224	0.000004	56	149	7.2	26.3	1.0872	80	0.70499	0.1655	5.1	80	5.4	577
K 149b	N Kozara	0.512844	0.000005	0.703838	0.000004	18	209	7.3	28.3	0.2491	80	0.70356	0.1560	4.0	80	4.4	624
K 150	N Kozara	0.512917	0.000004	0.703531	0.000004	5	238	2.8	9.8	0.0608	80	0.70346	0.1727	5.4	80	5.7	610

All given element concentrations were detected by ICP MS, except for Sm- and Nd-concentrations and isotope ratios of sample K135, which were detected by isotope dilution.

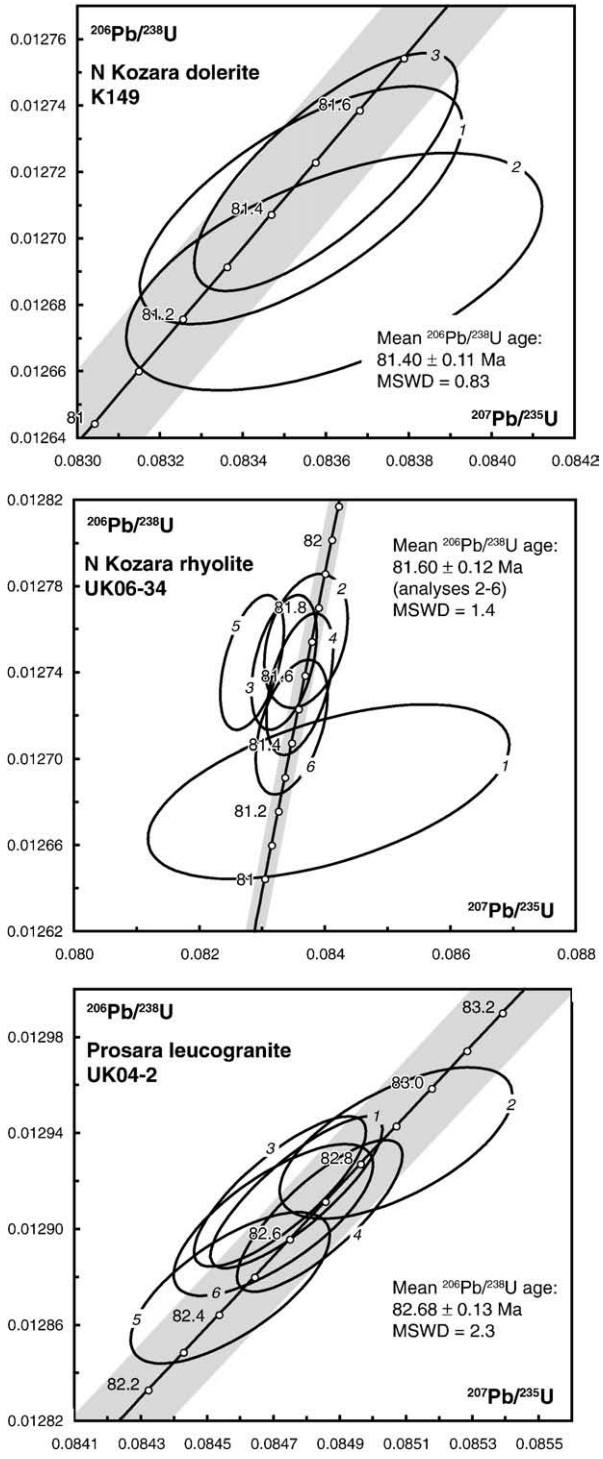

Fig. 11. Concordia diagrams showing the results of single zircon analyses from North Kozara and Prosara samples. Individual analyses are shown as 2σ error ellipses. Given ages are weighted mean $^{206}Pb/^{238}U$ ages. Grey shading indicates the uncertainties of the decay constants. See Figs. 4 and 12 for sample localities.

igneous part of the Western Vardar Ophiolitic Unit. Comparable ages were obtained from ophiolites in Albania (outside Fig. 12; see Fig. 2 in Dilek et al., 2008, for a recent compilation), from the frontal part of the obducted ophiolites (derived from the Western Vardar Zone according to Gawlick et al., 2008): a mafic dike from the Bulqiza Massif yielded a Rb–Sr biotite age of 158±4 Ma, equivalent to a K–Ar age of 160.5± 7.5 Ma (Tashko and Tërshana, 1988; cited in Dimo-Lahitte et al., 2001).

The mafic igneous rocks within the Greek ophiolites seem to be older. Gabbros and plagiogranites from the Vourinos complex (outside Fig. 12) yielded ages of 168.5±2.4 and 172.9±3.1 Ma, respectively, obtained by U–Pb ion-microprobe (SHRIMP) dating of zircons (Liati et al., 2004). The same study also reports ages of 171±3 Ma for gabbros from the Greek so-called "Pindos ophiolite" (in our view the frontal part of the obducted Western Vardar Ophiolitic Unit, see also Gawlick et al., 2008).

Most radiometric ages obtained from the Western Vardar Ophiolitic Unit are from amphibolites of the metamorphic sole (Lanphere et al., 1975; Okrusch et al., 1978; Lugović et al., 2006). The two K–Ar-ages obtained by Lanphere et al. (1975) for amphibolites from Konjuh (157±4 Ma) and Zlatibor (171±14 Ma) underwent a slight correction by Spray et al. (1984) on the basis of the new decay constant of Steiger and Jäger (1977) and thus became 161±4 and 178±14 Ma, respectively. Fig. 12 shows the corrected ages. Higher ages of 182–187 Ma were obtained from a metamorphic sole of the Eastern Vardar ophiolite at Razbojna (Karamata and Popević, unpubl.; in Karamata, 2006). The most recent age obtained for a metamorphic sole in the Dinarides is a pooled Sm–Nd isochron obtained with garnet, plagioclase, clinopyroxene, amphibole and whole rock on five granulites from Borja, which gave 171.4±3.7 Ma (Lugović et al., 2006). All ages regarding metamorphic sole formation in the former Yugoslavian sector of the Western Vardar Ophiolitic Unit are thus in agreement with those reported from the Albanian (159±2.6 to 171.7±1.7 Ma; Dimo-Lahitte et al., 2001) and Greek ophiolites (see Spray et al., 1984).

Within the analytical errors, the crystallisation age for the South Kozara gabbro (157.9±7.6 Ma) overlaps with the age of metamorphism or cooling of the geographically closest metamorphic soles (Borja 171.4±3.7 Ma; Konjuh 161±4 Ma). This suggests a rapid transition from seafloor spreading and associated MOR magmatism to intraoceanic subduction, which presumably occurred between the Bathonian and early Oxfordian (c. 166–157 Ma in the time-scale of Gradstein et al., 2004), as implied from the following line of reasoning. Growth of the dated minerals in the metamorphic soles occurred at a depth of c. 30–40 km according to thermobarometric estimates (Dimo-Lahitte et al., 2001). Given a subduction angle of 30° (young, hot, buoyant oceanic lithosphere entering subduction), this corresponds to a length of 60–80 km of subducted oceanic lithospheric slab. Hence, at a subduction velocity of, say, 5 cm a^{-1}, a metamorphic sole would have formed 1.2–1.6 Ma after subduction has started. This time span cannot be resolved with the available ages and their inherent analytical errors.

The age of the South Kozara gabbro is in conflict with the Hettangian to Late Bajocian age for the underlying ophiolitic mélange inferred by Babić et al. (2002), as the gabbro would be younger than the tectonically underlying mélange. Since the ages reported by Babić et al. (2002) give a maximum age of sedimentation of the matrix — the palynomorphs could even be reworked — we merely regard them as maximum ages for mélange formation related to obduction.

Radiometric ages from the ultramafic parts of the ophiolites are scarce. Fig. 12 shows a Sm–Nd isochron age of 146.8±3.7 Ma, obtained on a garnet-plagioclase-pyroxenite vein that cuts the dominantly lherzolithic peridotites of the Zlatibor massif (Bazylev et al., 2006 and pers. comm.). This age corresponds well with a pooled Sm–Nd-isochron age of 136±15 Ma (Fig. 6 in Lugović et al., 1991), constructed with clinopyroxenes and whole rock from lherzolites of three different localities (Borja, Konjuh and Zlatibor massifs; not shown in Fig. 12). Both ages are clearly younger than any of the adjacent metamorphic soles. It hence appears that the formation of oceanic lithosphere in parts of what presently constitutes the Western Vardar Ophiolitic Unit, that was in a suprasubdution position at that time, postdates the initiation of intraoceanic subduction but pre-dated final obduction (Fig. 13).

Another conclusion to be drawn from Fig. 12 is that Late Cretaceous magmatism is restricted to the Sava Zone. The U–Pb ages obtained on zircons from North Kozara (Fig. 11) correspond well with K–Ar whole-rock ages of 79 and 82 Ma obtained on dolerites from a sheeted dike complex near Gornji Podgradci (Lovrić, 1986; location given in Fig. 4).

Table 4
U–Pb isotopic data of analysed zircons from North Kozara and Prosara igneous rocks

Number[a]	Weight [mg]	Concentrations			Th/U[b]	Atomic ratios							Apparent ages			Error corr.
		U [ppm]	Pb rad. [ppm]	Pb nonrad [pg]		$^{206}Pb/^{204}Pb$[c]	$^{207}Pb/^{235}U$[d]	Error 2 s [%]	$^{206}Pb/^{238}U$[d]	Error 2 s [%]	$^{207}Pb/^{206}Pb$[d]	Error 2 s [%]	$^{206}Pb/^{238}U$	$^{207}Pb/^{235}U$	$^{207}Pb/^{206}Pb$	
Dolerite, North Kozara (K149)																
K149/1	0.0033	342	4.81	1.39	0.74	686	0.08354	0.38	0.01271	0.23	0.04768	0.28	81.40	81.47	83.50	0.68
K149/2	0.0015	502	7.25	1.30	0.85	494	0.08362	0.49	0.01269	0.23	0.04777	0.42	81.32	81.54	88.10	0.55
K149/3	0.0025	599	8.52	1.97	0.79	641	0.08360	0.31	0.01272	0.23	0.04767	0.20	81.49	81.53	82.60	0.76
K149/4	0.0046	34	0.44	2.55	0.48	68	0.08462	3.65	0.01254	0.33	0.04894	3.44	80.34	82.48	144.80	0.66
K149/5	0.0017	154	2.05	1.92	0.54	130	0.08345	2.35	0.01265	0.74	0.04785	2.12	81.03	81.38	91.70	0.45
Rhyolite, North Kozara (UK06-34)																
UK06-34/1	0.0033	134	1.78	4.47	0.51	100	0.08406	2.80	0.01268	0.26	0.04806	2.68	81.26	81.96	102.23	0.54
UK06-34/2	0.0025	143	1.92	1.41	0.55	228	0.08370	0.65	0.01275	0.20	0.04759	0.61	81.70	81.62	78.88	0.34
UK06-34/3	0.0009	579	7.75	0.98	0.55	456	0.08360	0.52	0.01273	0.21	0.04761	0.46	81.57	81.53	80.03	0.47
UK06-34/4	0.0018	222	2.97	0.79	0.55	437	0.08335	0.51	0.01274	0.20	0.04743	0.47	81.64	81.29	70.93	0.43
UK06-34/5	0.0015	488	6.52	0.82	0.55	752	0.08284	0.50	0.01274	0.20	0.04714	0.45	81.64	80.81	56.34	0.48
UK06-34/6	0.0016	622	8.28	2.83	0.53	306	0.08347	0.56	0.01271	0.20	0.04761	0.51	81.45	81.40	79.91	0.47
Alkalifeldspar granite, Prosara (UK04-2)																
UK04-2/1	0.0025	884	11.46	0.50	0.38	3739	0.08477	0.25	0.01292	0.20	0.04760	0.14	82.72	82.62	79.46	0.83
UK04-2/2	0.0023	1112	13.94	4.78	0.25	463	0.08507	0.34	0.01294	0.20	0.04770	0.26	82.85	82.90	84.38	0.63
UK04-2/3	0.0025	862	19.32	0.62	0.30	2959	0.08472	0.25	0.01292	0.20	0.04757	0.15	82.73	82.57	77.97	0.80
UK04-2/4	0.0025	1473	18.91	0.69	0.34	4534	0.08484	0.24	0.01291	0.20	0.04762	0.13	82.66	82.69	80.43	0.80
UK04-2/5	0.0020	875	11.20	0.89	0.34	1665	0.08457	0.29	0.01288	0.20	0.04764	0.21	82.47	82.43	81.40	0.69
UK04-2/6	0.0027	695	9.91	0.63	0.74	2529	0.08470	0.29	0.01290	0.20	0.04761	0.20	82.65	82.55	79.91	0.73

[a] All zircons annealed–leached (Mattinson, 2005).
[b] Calculated on the basis of radiogenic Pb^{208}/Pb^{206} ratios, assuming concordancy.
[c] Corrected for fractionation and spike.
[d] Corrected for fractionation, spike, blank and common lead (Stacey & Kramers, 1975).

Furthermore, they are in agreement with the biostratigraphic evidence (Karamata et al., 2000, 2005; our data). The tectonically higher unit in the northerly adjacent Prosara Mountain exposes a succession of greenschist-facies, mylonitic rhyolites and prasinites, followed up-section by metasandstones (see above). Based on the lithostratigraphic resemblance of the Prosara succession with that of North Kozara and the compatible U–Pb ages, we assigned it a Campanian age (Figs. 3 and 5). The greenschist- to lower amphibolite-grade succession exposed in Mount Motajica contains amphibolites overlain by calcite marbles. The protolith of the amphibolites could be mafic volcanics or volcaniclastics related to Campanian intraoceanic magmatism (Fig. 5).

Požeška Gora also shares great similarities with the North Kozara succession in terms of lithostratigraphy, igneous rock suite and ages. Late Cretaceous (to Early Paleogene) bimodal magmatism has furthermore been documented in numerous outcrops and oil wells in the Tisza Mega-Unit (Pamić, 1997; Pamić et al., 2000; see Fig. 2). The ages, obtained by K–Ar dating of whole-rock samples or amphibole concentrates, span a considerably wide range between c. 110 and 51 Ma (Pamić, 1997; Pamić et al., 2000). Excluding all samples reported as altered by Pamić et al. (2000), the age range reduces to c. 110 to 62 Ma. Basalts from the Voćin area (northern part of Papuk mountain, Fig. 2) are intercalated with sediments containing a Late Cretaceous microfauna (Pamić and Pécskay, 1994).

5.4. Paleotectonic significance of the Campanian igneous succession

Our data document the existence of Late Cretaceous intraoceanic magmatism and hence an area floored by oceanic lithosphere between the Adriatic and the Europe-derived Tisza and Dacia Mega-Units. Still unresolved is the question concerning the original tectonic position of the oceanic lithosphere that was subsequently subducted underneath the Europe-derived Tisza and Dacia Mega-Units in the latest Cretaceous. Was it a fragment of (a) the Neotethys, parts of which would have escaped Late Jurassic obduction onto the Adriatic passive margin or (b) part of the Alpine Tethys or (c) of both, the two being connected along the Sava Zone corridor? Option (a) is possibly in line with the reasoning of Karamata et al. (2000, 2005), who regarded the North Kozara igneous succession as representing a remnant oceanic area that remained open after parts of the Vardar Ocean had been obducted onto the Adriatic passive margin. This setting bears a close resemblance to the present-day situation in the Gulf of Oman. There, a remnant marine area, floored by oceanic crust, has remained open after the obduction of the Semail ophiolite onto the Arabian margin between c. 80 and 70 Ma (Coleman, 1981; see also Fig. 3.28 in Nicolas, 1989). At present, this remnant oceanic branch in the Gulf of Oman is being subducted underneath the Makran accretionary wedge to the north.

The closure of the remnant oceanic area in what is now the Sava Zone must have occurred stepwise (Fig. 13). An earlier step involved Campanian intraoceanic magmatism, possibly forming on Jurassic-age oceanic lithosphere of the Vardar Ocean that had escaped obduction onto the Adriatic passive margin (Fig. 13a). We leave it open, whether this Campanian intraoceanic magmatism occurred in an ocean-island (Fig. 13, "b1") or back-arc basin setting (Fig. 13, "b2"). A later step involved the installation of a more internally positioned subduction (Fig. 13c), which ultimately led to the closure of this oceanic branch by Maastrichtian to early Paleogene times. Greenschist-facies metamorphism in the formations exposed in the Prosara, Motajica and Požeška Gora areas suggests that the Late Cretaceous igneous succession positioned more internally in respect to North Kozara became involved in thrusting and deep burial after collision. By contrast, the lack of a metamorphic overprint in the Mesozoic cover of Psunj–Papuk Mountains shows that the Tisza Mega-Unit occupied an upper-plate position during this closure. The widespread occurrence of Late Cretaceous (to Early Paleogene) subduction-related bimodal volcanics in the Tisza Mega-Unit itself (Pamić, 1993b, 1997; Pamić et al., 2000) suggests the installation of a continental volcanic arc on top of the upper plate above a north-dipping subduction zone. This magmatism might be considered as a prolongation of the "banatite" belt of Bulgaria, Serbia and Romania.

Possibility (b) is unlikely given the fact that subduction of the Alpine Tethys slab in the Alps during Late Cretaceous to Early Palaeogene times was south-directed, and hence opposed to the northeast-directed subduction inferred for the Sava Zone. Possibility (c) cannot be excluded

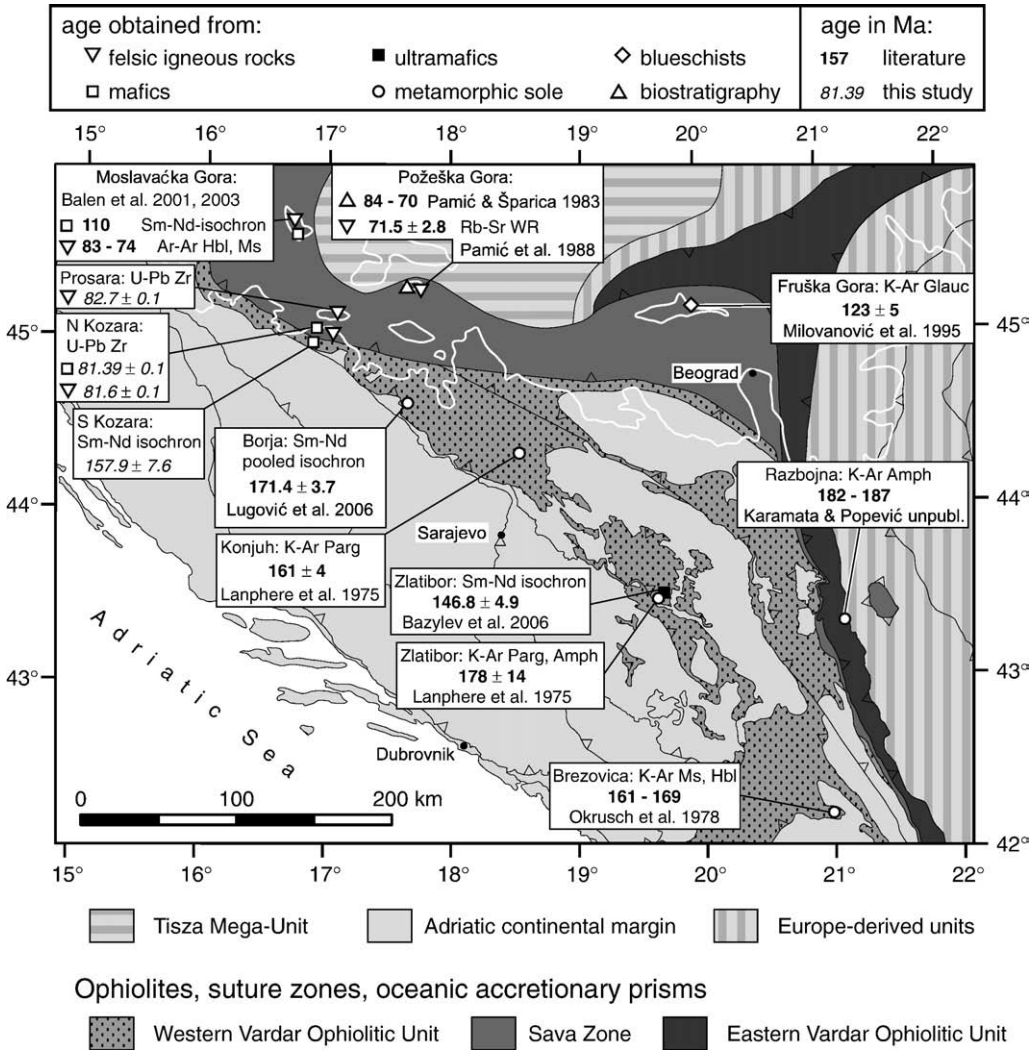

Fig. 12. Compilation of radiometric ages from the Western Vardar Ophiolitic Unit and the Sava Suture Zone. Ages from igneous rocks are interpreted as crystallisation ages. Ages from peridotites are considered as formation ages of the oceanic lithosphere. Ages from metamorphic sole rocks and blueschists are formation or cooling ages. The original ages of Lanphere et al. (1975) were corrected by Spray et al. (1984) to match the new decay constants of Steiger and Jäger (1977). Mineral abbreviations: Amph = amphibole, Glauc = glaucophane, Hbl = hornblende, Ms = muscovite, Parg = pargasite, WR = whole rock, Zr = zircon.

however, for the following reason, discussed in more detail in Schmid et al. (2008): In order to account for the late Mesozoic to Cenozoic northward drift of the Adriatic Plate, the Alpine Tethys must have been spatially connected eastwards to a northwestern-most, still open branch of Neotethys. Such a link may indeed have existed in the area of the Sava Zone of Northern Bosnia. However, it should be noted that in a structural sense, the Sava Zone is definitely part of Tertiary collision in the Dinarides. The polarity of subduction probably changed somewhere along the present-day Mid-Hungarian Fault Zone ENE of Zagreb (Márton et al., 2007; Tischler et al., 2007).

The bimodal volcanics of the northernmost internal Dinarides (Pamić, 1997; Pamić et al., 2000) have already been suggested as a potential source area of volcanic ash layers found in the Late Cretaceous of the Central Apennines (Bernoulli et al., 2004). The radiometric ages reported here strongly support this hypothesis.

6. Conclusions

1.) Campanian to Early Maastrichtian intra-oceanic magmatism is reported in several inselbergs in the Sava Zone and implies that the Adriatic and Europe-derived smaller plates (such as the Tisza and the Dacia Mega-Unit) were still separated by a deep basin floored by oceanic lithosphere at this time. The earliest possible timing for the collision of these plates is hence the latest Cretaceous.
2.) Final closure of the oceanic fragment was the consequence of subduction of the Dinarides underneath the Tisza Mega-Unit representing the upper plate.
3.) Late Cretaceous to Early Paleogene bimodal volcanism in the Tisza Mega-Unit is attributed to the formation of a continental volcanic arc located in the upper plate during subduction. The end of subduction is marked by both the cessation of volcanic activity and the end of turbidite sedimentation in the Sava Zone in the Paleocene to Eocene.
4.) The Campanian to Early Maastrichtian oceanic crust can be considered as a northwestern-most extension of the Vardar Ocean, which at the same time was linked with the Alpine Tethys in the investigated area.

Acknowledgments

Stevan Karamata (Beograd) made us aware of the location and importance of the splendid outcrop of Campanian pillows and Scaglia Rossa in North Kozara. We are also deeply indebted to Michèle Caron (Fribourg) for her generous help with biostratigraphic determinations. Fred Gaidies and Cédric Rettenmund (Basel) performed whole rock XRF analyses. Monika Jelenc (Vienna) is thanked for help in measuring

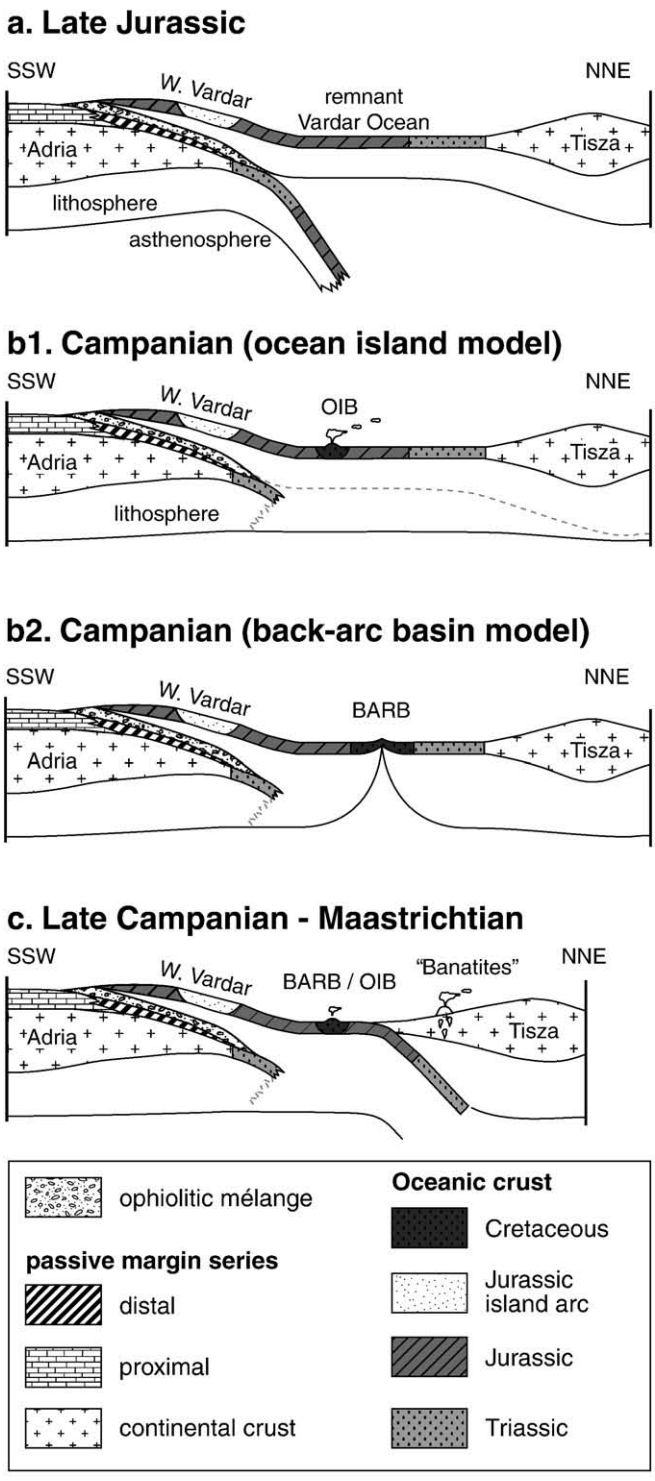

Fig. 13. Schematic sketches illustrating the invoked geodynamic evolution of the northern, E–W trending part of the Sava Suture Zone (not to scale). a: after Late Jurassic obduction of the Western Vardar Ophiolitic Unit onto the Adriatic passive margin, b: Campanian intraoceanic magmatism, c: before final ocean closure and subsequent collision of the Adriatic plate and the Tisza Mega-Unit.

Sr- and Nd-isotopes. The help of Maria Ovtcharova (Geneva) for U–Pb age determinations is also kindly acknowledged. Hazim Hrvatović (Sarajevo) is greatly thanked for logistic and scientific support. Thorough and very constructive reviews by Vladica Cvetković (Beograd), Alastair Robertson (Edinburgh) and Bruno Tomljenović (Zagreb), as well as additional helpful comments by Milica Božović (Mainz) and Sun-Lin Chung (Taipei) helped in further improving the manuscript. Greg Shellnutt (Taipei) refined the English. Financial support for the Basel group through the Swiss National Science Foundation (projects "Tisza" Nrs. 200021-101883/1 and 200020-109278/1) is kindly acknowledged.

Appendix A1. Analytical techniques

A1.1. Whole rock major and trace element analyses

The analysed samples presented in this study consist of two different subsets that were collected during separate field campaigns. Whole rock (WR) analyses of the two subsets were performed separately in different laboratories before combining the results into one dataset for the present study. One subset consists of samples collected by B. Lugović (sample labels starting with "KO-", Table 3). The other sample subset was collected by K. Ustaszewski between 2004 and 2006 (sample labels starting with "K", followed by a three-digit number, Table 3). Analytical techniques are described below.

Sample subset "KO-" (sampled by B. Lugović)

Bulk-rock powders for chemical analyses were obtained from rock chips free of visible veins and weathering surfaces. Major elements and trace elements Rb, Ba, Sr, Zr, Cr and Ni were measured by wavelength dispersive X-ray fluorescence analysis (WD-XRFA) on fused and pressed pellets using conventional techniques. Trace elements Th, U, Nb, Ta, Hf, Y and REE were analysed by ICP-MS at Actlab Laboratories in Toronto, Canada. Trace elements were determined from diluted solution after leaching 500 mg sample in 3 ml HCl–HNO_3–H_2O at 95 °C for 1 h and REE were analysed after $LiBO_2$/$Li_2B_4O_7$ fusion of 200 mg sample.

Sample subset "K" (sampled by K. Ustaszewski)

Bulk-rock powders for chemical analyses were obtained from fresh specimens devoid of weathering surfaces. Major element concentrations were obtained from glass pellets by WD-XRFA using a Bruker AXS SRS-3400 at the Mineralogical and Petrographical Institute, University of Basel. Trace element concentrations were determined by ICP-MS on a Perkin Elmer 5000 at the Service d'Analyse des Roches et des Minéraux of the CNRS-CRPG Nancy, France (http://www.crpg.cnrs-nancy.fr/SARM).

A1.2. Isotopic analyses

Sm–Nd and Sr isotope analyses were performed at the Department of Geological Sciences at the University of Vienna. Sample weights of handpicked mineral separates used for dissolution were about 100 mg. The chemical sample preparation followed the procedure described by Sölva et al. (2005). Spiked Sm and Nd ratios were measured at a Finnigan® MAT 262, whereas unspiked Nd and Sr ratios were analysed at a ThermoFinnigan® Triton TI TIMS. All elements were run from Re double filaments. On the Triton TI the La Jolla standard yielded $^{143}Nd/^{144}Nd = 0.511846 \pm 2$ ($n = 7$) whereas $^{86}Sr/^{87}Sr = 0.710246 \pm 2$ ($n = 7$) were determined for the NBS987.

A1.3. U–Pb dating

Zircons were prepared by standard mineral separation techniques (crushing, milling, concentration via Wilfey table, magnetic separation and heavy liquid separation in methylene iodide (density > 3.1 g cm^{-3})). Suitable grains were then handpicked in ethanol under a binocular microscope. In order to minimise the effects of secondary lead-loss, the chemical abrasion "CA-TIMS" technique, involving high-temperature annealing followed by a subsequent HF leaching step (Mattinson, 2005) was applied. Isotopic analyses were performed at the Department of Earth Sciences at the University of Geneva. The analytical techniques are described in Ovtcharova et al. (2006) in more detail. Calculation of $^{206}Pb/^{238}U$ ages was done with the Isoplot/Ex v.3 program (Ludwig, 2005).

Appendix A2. Supplementary data

Supplementary data associated with this article can be found, in the online version, at doi:10.1016/j.lithos.2008.09.010.

References

Babić, L., Hochuli, P., Zupanić, J., 2002. The Jurassic ophiolitic mélange in the NE Dinarides: dating, internal structure and geotectonic implications. Eclogae Geologicae Helvetiae 95, 263–275.

Balen, D., Schuster, R., Garašić, V., 2001. A new contribution to the geochronology of Mt. Moslavačka Gora (Croatia). In: Ádam, A., Szarka, L., Szendrői, J. (Eds.), PANCARDI 2001. Geodetic and Geophysical Research Institute of the Hungarian Academy of Science, Sopron, Hungary, pp. DP–2.

Balen, D., Schuster, R., Garašić, V., Majer, V., 2003. The Kamenjača Olivine gabbro from Moslavačka Gora (South Tisia, Croatia). Rad Hrvatske akademije znanosti i umjetnosti 486 (27), 57–76.

Balen, D., Horváth, P., Tomljenović, B., Finger, F., Humer, B., Pamić, J., Árkai, P., 2006. A record of pre-Variscan Barrovian regional metamorphism in the eastern part of the Slavonian Mountains (NE Croatia). Mineralogy and Petrology 87, 143–162.

Bazylev, B., Zakariadze, G., Popević, A., Kononkova, N., Karpenko, S., Simakin, S., 2006. Spinel peridotites and garnet pyroxenites from Bistrica massif (Dinaridic ophiolite belt): the possible fragment of a sub-continental mantle. International Symposium on the Mesozoic ophiolite belts of the northern part of the Balkan Peninsula. Serbian Academy of Sciences and Arts, Commitee of Geodynamics, Belgrade, pp. 12–14. May 31st–June 6th, 2006.

Belak, M., Halamić, J., Marchig, V., Tibljas, D., 1998. Upper Cretaceous–Palaeogene tholeiitic basalts of the southern margin of the Pannonian Basin: Požeška Gora Mt. (Croatia). Geologia Croatica 51, 163–174.

Bernoulli, D., Laubscher, H., 1972. The palinspastic problem of the Hellenides. Eclogae Geologicae Helvetiae 65, 107–118.

Bernoulli, D., Schaltegger, U., Stern, W.B., Frey, M., Caron, M., Monechi, S., 2004. Volcanic ash layers in the Upper Cretaceous of the Central Apennines and a numerical age for the early Campanian. International Journal of Earth Sciences 93, 384–399.

Boynton, W.V., 1984. Cosmochemistry of the rare earth elements: meteorite studies. In: Henderson, P. (Ed.), Rare Earth Element Geochemistry, Development in Geochemistry. Elsevier, Amsterdam, pp. 63–114.

Cameron, W.E., Nisbet, E.G., Dietrich, V.J., 1979. Boninites, komatiites and ophiolitic basalts. Nature 280, 550–553.

Coleman, R.G., 1981. Tectonic setting for ophiolite obduction in Oman. Journal of Geophysical Research 86, 2497–2508.

Crawford, A.J., Beccaluva, L., Serri, G., 1981. Tectono-magmatic evolution of the West Philippine-Mariana region and the origin of boninites. Earth and Planetary Science Letters 54, 346–356.

Dilek, Y., Furnes, H., Shallo, M., 2008. Geochemistry of the Jurassic Mirdita Ophiolite (Albania) and the MORB to SSZ evolution of a marginal basin oceanic crust. Lithos 100, 174–209.

Dimitrijević, M.D., 1997. Geology of Yugoslavia. Geological Institute GEMINI, Beograd. 190 pp.

Dimitrijević, M.D., 2001. Dinarides and the Vardar Zone: a short review of the geology. Acta Vulcanologica 13, 1–8.

Dimo-Lahitte, A., Monié, P., Vergély, P., 2001. Metamorphic soles from the Albanian ophiolites: Petrology, $^{40}Ar/^{39}Ar$ geochronology, and geodynamic evolution. Tectonics 20, 78–96.

Djerić, N., Vishnevskaya, V.S., 2006. Some Jurassic to Cretaceous radiolarians of Serbia, Mesozoic Ophiolite Belt of the Northern Part of the Balkan Peninsula, pp. 29–36. Belgrade-Banja Luka, 31. 05.–06. 06. 2006.

Djerić, N., Vishnevskaya, V.S., Schmid, S.M., 2007. New data on radiolarians from the Dinarides (Bosnia and Serbia). Abstract Volume 8th Workshop on Alpine Geological Studies Davos, pp. 17–19.

Djerković, B., Djordjević, D., Hohrajn, J., Jojić, D., Jurić, M., Kačar, B., Kapeler, I., Kovačević, R., Kujundžić, S., Ložajić-Maglov, M., Maksimčev, S., Marić, L., Pamić, J., Sunarić-Pamić, O., Vejlović, R., Vilovski, S., 1975. Basic geological map sheet of Yugoslavia 1:100.000, sheet Prijedor L 33-118. Federal Geological Institute Beograd.

Gawlick, H.-J., Frisch, W., Hoxha, L., Dumitrica, P., Krystyn, L., Lein, R., Missoni, S., Schlagintweit, F., 2008. Mirdita Zone ophiolites and associated sediments in Albania reveal Neotethys Ocean origin. International Journal of Earth Sciences 97, 865–881.

Georgiev, G., Dabovski, C., Stanisheva-Vassileva, G., 2001. East-Srednogorie–Balkan Rift Zone. In: Ziegler, P.A., Cavazza, W., Robertson, A.H.F., Crasquin-Soleau, S. (Eds.), Peri-Tethys Memoir 6: Peri-Tethyan Rift/Wrench Basins and Passive Margins. Mémoires du Muséum National d'Histoire Naturelle Paris, pp. 259–293.

Gill, J., 1981. Orogenic Andesites and Plate Tectonics. Minerals and Rocks, vol. 16. Springer Verlag, Berlin. 390 pp.

Gradstein, F., Ogg, J., Smith, A.G., 2004. A Geologic Time Scale. Cambridge University Press, Cambridge. 589 pp.

Heinrich, C.A., Neubauer, F., 2002. Cu–Au–Pb–Zn–Ag metallogeny of the Alpine-Balkan-Carpathian-Dinaride geodynamic province. Mineralium Deposita 37, 533–540.

Hickey, R.L., Frey, F.A., 1982. Geochemical characteristics of boninite series volcanics. implications for their source. Geochimica et Cosmochimica Acta 46, 2099–2115.

Hofmann, A.W., 1988. Chemical differentiation of the Earth: the relationship between mantle, continental crust, and oceanic crust. Earth and Planetary Science Letters 90, 297–314.

Hofmann, A.W., 1997. Mantle geochemistry: the message from oceanic volcanism. Nature 385, 219–229.

Jelaska, V., 1981. Facial characteristics of the Mt. Kozara flysch (North Bosnia) (in Croatian with English summary). Vesnik, Serija A: Geologija 38/39, 137–145.

Jovanović, C., Magaš, N., 1986. Basic geological map sheet of Yugoslavia 1:100.000, sheet Kostajnica L 33-106. Federal Geological Institute Beograd.

Karamata, S., 2006. The geological development of the Balkan Peninsula related to the approach, collision and compression of Gondwanan and Eurasian units. In: Robertson, A.H.F., Mountrakis, D. (Eds.), Tectonic Development of the Eastern Mediterranean Region. Geological Society Special Publications. Geological Society of London, London, pp. 155–178.

Karamata, S., Olujić, J., Protić, L., Milovanović, D., Vujnović, L., Popević, A., Memović, E., Radovanović, Z., Resimić-Sarić, K., 2000. The western belt of the Vardar Zone — the remnant of a marginal sea. In: Karamata, S., Jankovic, S. (Eds.), International Symposium Geology and metallogeny of the Dinarides and the Vardar zone, Banja Luka, Sarajevo, pp. 131–135.

Karamata, S., Sladić-Trifunović, M., Cvetković, V., Milovanović, D., Šarić, K., Olujić, J., Vujnović, L., 2005. The western belt of the Vardar Zone with special emphasis to the ophiolites of Podkozarje — the youngest ophiolitic rocks of the Balkan Peninsula. Bulletin T. CXXX de l'Académie serbe des sciences et des arts. Classe des Sciences mathémathiques et naturelles 43, 85–96.

Kim, J., Jacobi, R.D., 2002. Boninites: characteristics and tectonic constraints, north-eastern Appalachians. Physics and Chemistry of the Earth 27, 109–147.

Krenn, E., Ustaszewski, K., Finger, F., 2008. Detrital and newly formed metamorphic monazite in amphibolite-facies metapelites from the Motajica Massif, Bosnia. Chemical Geology 254, 164–174. doi:10.1016/j.chemgeo.2008.03.012.

Lanphere, M., Coleman, R.G., Karamata, S., Pamić, J., 1975. Age of amphibolites associated with Alpine peridotites in the Dinaride ophiolite zone, Yugoslavia. Earth and Planetary Science Letters 26, 271–276.

Le Bas, M.J., Le Maitre, R.W., Streckeisen, A.L., Zanettin, B., IUGS Subcommission on the Systematics of Igneous Rocks, 1986. A chemical classification of volcanic rocks based on the total alkali-silica diagram. Journal of Petrology 27, 745–750.

Liati, A., Gebauer, D., Fanning, C.M., 2004. The age of ophiolitic rocks of the Hellenides (Vourinos, Pindos, Crete): first U–Pb ion microprobe (SHRIMP) zircon ages. Chemical Geology 207, 171–188.

Lovrić, A., 1986. Ages of Magmatic and Metamorphic Rocks by Isotopic Methods (in Serbian), Bulletin of the Fund for Scientific Investigations. Serbian Academy of Sciences and Arts, Beograd, p. 18.

Ludwig, K., 2005. Isoplot/Ex v.3, USGS Open File report.

Lugović, B., Altherr, R., Raczek, I., Hofmann, A.W., Majer, V., 1991. Geochemistry of peridotites and mafic igneous rocks from the Central Dinaric Ophiolite Belt, Yugoslavia. Contributions to Mineralogy and Petrology 106, 201–216.

Lugović, B., Šegvić, B., Babajić, E., Trubelja, F., 2006. Evidence for short-living intraoceanic subduction in the Central Dinarides, Konjuh Ophiolite Complex (Bosnia–Hercegovina). International Symposium on the Mesozoic Ophiolite Belts of the Northern Part of the Balkan Peninsula. Serbian Academy of Sciences and Arts, Commitee of Geodynamics, Belgrade, pp. 72–75. May 31st–June 6th, 2006.

Mahlburg Kay, S., Godoy, E., Kurtz, A., 2005. Episodic arc migration, crustal thickening, subduction erosion, and magmatism in the south-central Andes. Geological Society of America Bulletin 117, 67–88.

Márton, E., Tischler, M., Csontos, L., Fügenschuh, B., Schmid, S., 2007. The contact zone between the ALCAPA and Tisza-Dacia mega-tectonic units of Northern Romania in the light of new paleomagnetic data. Swiss Journal of Geosciences 100, 109–124.

Mattinson, J.M., 2005. Zircon U–Pb chemical abrasion ("CA-TIMS") method: combined annealing and multi-step partial dissolution analysis for improved precision and accuracy of zircon ages. Chemical Geology 220, 47–66.

Milovanović, D., Marchig, V., Karamata, S., 1995. Petrology of the crossite schist from Fruška Gora Mts (Yugoslavia), relic of a subducted slab of the Tethyan oceanic crust. Journal of Geodynamics 20, 289–304.

Mojićević, M., Vilovski, S., Tomić, B., 1976. Basic geological map sheet of Yugoslavia 1:100.000, sheet Banja Luka L 33-119. Federal Geological Institute, Sarajevo.

Murphy, J.B., 2007. Igneous Rock Associations 8: Arc Magmatism II: geochemical and isotopic characteristics. Geoscience Canada 34, 7–36.

Neubauer, F., Heinrich, C.A., GEODE ABCD Working Group, 2003. Late Cretaceous and Tertiary geodynamics and ore deposit evolution of the Alpine-Balkan-Carpathian-Dinaride orogen. In: Eliopoulos, D.G. et al., (Eds.), Mineral Exploration and Sustainable Development. Proceedings of the Seventh Biennial Society for Geology Applied to Mineral Deposits Meeting on Mineral Exploration and Sustainable Development, Athens, Greece. Millpress Science Publishers, Rotterdam, pp. 1133–1136. August 24–28, 2003.

Nicolas, A., 1989. Structures of Ophiolites and Dynamics of Oceanic Lithosphere. Petrology and Structural Geology, 4. Kluwer Academic Publishers, Dordrecht. 367 pp.

Okrusch, M., Seidel, E., Kreuzer, H., Harre, W., 1978. Jurassic age of metamorphism at the base of the Brezovica peridotite (Yugoslavia). Earth and Planetary Science Letters 39, 291–297.

Ovtcharova, M., Bucher, H., Schaltegger, U., Galfetti, T., Brayard, A., Guex, J., 2006. New Early to Middle Triassic U–Pb ages from South China: calibration with ammonoid biochronozones and implications for the timing of the Triassic biotic recovery. Earth and Planetary Science Letters 243, 463–475.

Pamić, J., 1993a. Eoalpine to Neoalpine magmatic and metamorphic processes in the northwestern Vardar Zone, the easternmost Periadriatic Zone and the south-western Pannonian Basin. Tectonophysics 226, 503–518.

Pamić, J., 1993b. Late Cretaceous volcanic rocks from some oil wells in the Drava depression and adjacent mountains of the southern parts of the Pannonian Basin (North Croatia). Nafta 44, 203–210.

Pamić, J., 1997. Volcanic rocks of the Sava–Drava interfluve and Baranja (in Croatian with English summary). Nafta, 8, Zagreb. 192 pp.

Pamić, J., 2002. The Sava–Vardar Zone of the Dinarides and Hellenides versus the Vardar Ocean. Eclogae Geologicae Helvetiae 95, 99–113.

Pamić, J., Šparica, M., 1983. The age of the volcanic rocks of Požeška Gora (Croatia, Yugoslavia). In Croatian with English abstract. Rad Jugosl. Akad. znan. umjet. 404, 183–198.
Pamić, J., Prohić, E., 1989. Novi prilog petroloskom poznavanju alpinskih granitnih i metamorfnih stijena Motajice u sjevernim Dinaridima u Bosni. (A new contribution to the petrology of Alpine granite and metamorphic rocks from Motajica Mt. in the northernmost Dinarides, Yugoslavia). Geološki Glasnik 13, 145–176.
Pamić, J., Pécskay, Z., 1994. Geochronology of Upper Cretaceous and Tertiary igneous rocks from the Slavonija–Srijem Depression. Nafta 45, 331–339.
Pamić, J., Lanphere, M., McKee, E., 1988. Radiometric ages of metamorphic and associated igneous rocks of the Slavonian Mountains in the southern part of the Pannonian Basin, Yugoslavia. Acta Geologica 18, 13–39.
Pamić, J., Árkai, P., O'Neil, J., Antai, C., 1992. Very low- and low-grade progressive metamorphism of Upper Cretaceous sediments of Mt. Motajica, northern Dinarides, Yugoslavia. In: Vozar, J. (Ed.), Special Volume to the Problems of the Paleozoic Geodynamic Domains; Western Carpathians, Eastern Alps. Dionýz Stur Institute of Geology, Bratislava, pp. 131–146.
Pamić, J., Belak, M., Bullen, T.D., Lanphere, M.A., McKee, E.H., 2000. Geochemistry and geodynamics of a Late Cretaceous bimodal volcanic association from the southern part of the Pannonian Basin in Slavonija (Northern Croatia). Mineralogy and Petrology 68, 271–296.
Pamić, J., Tomljenović, B., Balen, D., 2002. Geodynamic and petrogenetic evolution of Alpine ophiolites from the central and NW Dinarides: an overview. Lithos 65, 113–142.
Pantić, N., Jovanović, O., 1970. On the age of "Azoic" or "Palaeozoic slates" in Motajica Mountain based on microfloristic remnants (in Serbocroatian with English abstract). Geološki Glasnik 14, 190–214.
Ricou, L.E., 1994. Tethys reconstructed: plates, continental fragments and their boundaries since 260 Ma from Central America to South-eastern Asia. Geodinamica Acta 7, 169–218.
Robertson, A.H.F., Karamata, S., 1994. The role of subduction–accretion processes in the tectonic evolution of the Mesozoic Tethys in Serbia. Tectonophysics 234, 73–94.
Săndulescu, M., Visarion, M., 1977. Considérations sur la structure tectonique du soubassement de la dépression de Transylvanie. Dări de seamă ale şedinţelor 66, 153–173.
Schefer, S., Fügenschuh, B., Schmid, S.M., Egli, D., Ustaszewski, K., 2007. Tectonic evolution of the suture zone between Dinarides and Carpatho-Balkan: field evidence from the Kopaonik region, southern Serbia, EGU General Assembly 2007. Geophysical Research Abstracts 03891 Vienna.
Schilling, J.G., Zajac, M., Evans, R., Johnston, T., White, W., Devine, J.D., Kingsley, R., 1983. Petrologic and geochemical variations along the Mid-Atlantic Ridge from 29 degrees N to 73 degrees N. American Journal of Science 283, 510–586.
Schmid, S.M., Bernoulli, D., Fügenschuh, B., Matenco, L., Schefer, S., Schuster, R., Tischler, M., Ustaszewski, K., 2008. The Alpine–Carpathian–Dinaridic orogenic system: compilation and evolution of tectonic units. Swiss Journal of Geosciences 101, 139–183.
Shand, S.J., 1947. Eruptive Rocks. Their Genesis, Composition, Classification, and Their Relation to Ore-Deposits, with a Chapter on Meteorite. John Wiley & Sons, New York. 488 pp.
Smith, A.G., Spray, J.G., 1984. A half-ridge transform model for the Hellenic–Dinaric ophiolites. In: Dixon, J.E., Robertson, A.H.F. (Eds.), The geological evolution of the Eastern Mediterranean. Geological Society Special Publications, vol. 17. Blackwell Scientific Publications, pp. 629–644.
Sölva, H., Grasemann, B., Thöni, M., Thiede, R., Habler, G., 2005. The Schneeberg Normal Fault Zone: normal faulting associated with Cretaceous SE-directed extrusion in the Eastern Alps (Italy/Austria). Tectonophysics 401, 143–166.
Šparica, M., Bužaljko, R., Jovanović, C., 1980. Basic geological map sheet of Yugoslavia 1:100.000, sheet Nova Kapela L 33-108. Federal Geological Institute Beograd.
Šparica, M., Bužaljko, R., Jovanović, C., 1984. Basic geological map sheet of Yugoslavia 1:100.000, sheet Nova Gradiška L 33-107. Federal Geological Institute Beograd.
Spray, J.G., Bébien, J., Rex, D.C., Roddick, J.C., 1984. Age constraints on the igneous and metamorphic evolution of the Hellenic–Dinarides ophiolites. In: Dixon, J.E., Robertson, A.H.F. (Eds.), The Geological Evolution of the Eastern Mediterranean. Geological Society Special Publication, vol. 17. Blackwell Scientific Publications, pp. 619–627.
Stacey, J.S., Kramers, J.D., 1975. Approximation of terrestrial lead isotope evolution by a two-stage model. Earth and Planetary Science Letters 26, 207–221.
Starijaš, B., Balen, D., Tiblaš, D., Schuster, R., Humer, B., Finger, F., 2004. The Moslavačka Gora Massif in Croatia: part of a Late Cretaceous high-heat-flow zone in the Alpine-Balkan-Carpathian-Dinaride collision belt, Pangeo Austria 2004: "Erdwissenschaften und Öffentlichkeit". Berichte des Institutes für Erdwissenschaften der Karl-Franzens Universität Graz, Graz, pp. 453–454.
Starijaš, B., Gerdes, A., Balen, D., Tibljaš, D., Schuster, R., Mazer, A., Humer, B., Finger, F., 2006. Geochronology, metamorphic evolution and geochemistry of granitoids of the Moslavačka Gora Massif (Croatia). Congress of the Carpathian–Balkan Geological Association, Beograd (Serbia), pp. 594–597.
Steiger, R.H., Jäger, E., 1977. Subcommission on geochronology: convention on the use of decay constants in geo- and cosmochronology. Earth and Planetary Science Letters 36, 359–362.
Sun, C.H., Stern, R.J., 2001. Genesis of Mariana shoshonites: contribution of the subduction component. Journal of Geophysical Research 106, 589–608.
Tari-Kovačić, V., Mrinjek, E., 1994. The Role of Palaeogene Clastics in the Tectonic Interpretation of Northern Dalmatia (Southern Croatia). Geologia Croatica 47, 127–138.
Tashko, A., Tërshana, A., 1988. Mafic segregations with phlogopite in the Bulqiza Massif (English Translation). Bull. Shkencave. Gjeol. 2, 87–95.
Tischler, M., Gröger, H., Fügenschuh, B., Schmid, S., 2007. Miocene tectonics of the Maramures area (Northern Romania): implications for the Mid-Hungarian fault zone. International Journal of Earth Sciences 96, 473–496.
von Quadt, A., Moritz, R., Peytcheva, I., Heinrich, C.A., 2005. 3: Geochronology and geodynamics of Late Cretaceous magmatism and Cu–Au mineralization in the Panagyurishte region of the Apuseni–Banat–Timok–Srednogorie belt, Bulgaria. Ore Geology Reviews 27, 95–126.
Winter, J.D., 2001. An introduction to igneous and metamorphic petrology. Prentice–Hall, Upper Saddle River, New Jersey. 697 pp.